World Journal of Microbiology and Biotechnology (2026) 42:63
https://doi.org/10.1007/s11274-026-04798-0

RESEARCH

Biohealing through biocalcification by urolytic bacteria *Bacillus subtilis* ATCC 6633 on marble surfaces

Turkan Dal Bicer[1] · Seval Cing Yildirim[1] · Fadime Nulufer Kivilcim[2] · Ahmet Gultek[2]

Received: 27 December 2024 / Accepted: 10 January 2026
© The Author(s) 2026

Abstract

This study investigates the biocalcification potential of *Bacillus subtilis* ATCC 6633, a ureolytic bacterium, for the biohealing of marble surfaces through calcium carbonate ($CaCO_3$) precipitation. Comparative experiments were conducted using live and dead bacterial cells on CO_2-pre-treated and untreated marble samples, with calcium chloride and calcium acetate employed as calcium sources, to evaluate their effects on crystal polymorphism and surface modification. The results show that bacterial viability and calcium source jointly influence mineral phase formation, with live cells predominantly promoting the formation of stable calcite and aragonite, whereas dead cells and calcium acetate favor the formation of metastable vaterite. Microstructural and mineralogical analyses using scanning electron microscopy (SEM), energy-dispersive X-ray spectroscopy (EDX), X-ray diffraction (XRD), and atomic force microscopy (AFM) confirmed substantial $CaCO_3$ deposition on marble surfaces. AFM measurements indicated a reduction in maximum pore depth, defined as the vertical height difference between pore bottoms and the surrounding marble surface, from 35.00 ± 7.07 μm in control samples to 22.50 ± 8.20 μm in biocalcified samples, reflecting partial filling of pores and cracks. In addition, micropores (0.02–0.03 mm) were fully filled, while macropores (3–5 mm) were partially occluded by crystalline deposits. CO_2 pre-treatment enhanced surface carbon availability and promoted more uniform $CaCO_3$ nucleation, as supported by SEM-EDX and XRD analyses. Overall, these findings indicate that microbially induced carbonate precipitation (MICP), combined with appropriate surface preconditioning and calcium source selection, represents a potential and sustainable strategy for marble conservation and related bio-construction applications.

✉ Seval Cing Yildirim
seval.cing@inonu.edu.tr

[1] Department of Biology, Science and Art Faculty, University of Inonu, Malatya, Turkey

[2] Department of Chemistry, Science and Art Faculty, University of Inonu, Malatya, Turkey

Published online: 27 January 2026

Graphical abstract

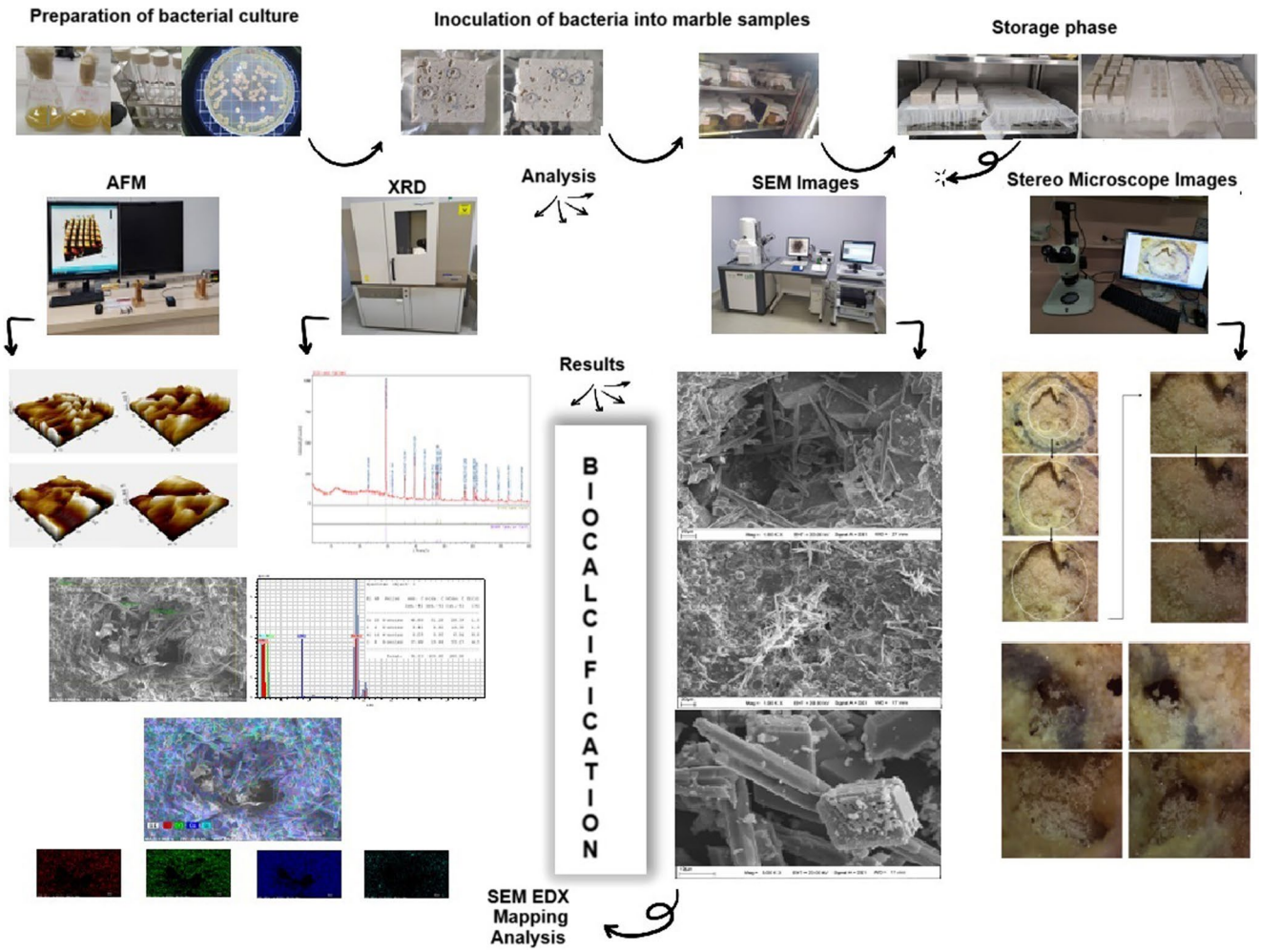

Highlights

- Microbial calcite seals microcracks, redefining marble conservation.
- Calcium source dictates crystal fate: calcite, aragonite, or vaterite.
- Sustainable biocalcification transforms marble restoration practices.

Keywords Microbially induced carbonate precipitation (MICP) · *Bacillus subtilis* ATCC 6633 · Marble biohealing · Crystal polymorphism · CO_2 pre-treatment

Introduction

Biohealing represents an emerging strategy in material science and conservation, leveraging the metabolic activity of microorganisms to repair and reinforce structural materials. Among these, biocalcification—a process driven by urea-hydrolyzing bacteria such as *Bacillus subtilis* has gained attention for its ability to induce calcium carbonate ($CaCO_3$) precipitation on mineral surfaces (Rajasekar et al. 2024; Sreekala et al. 2024). This bacterium metabolizes urea into carbonate ions, promoting calcite crystal formation, particularly on marble. By harnessing such microbial pathways, biohealing not only mitigates deterioration caused by environmental stressors but also enhances the durability and sustainability of marble-based architectural heritage. This interdisciplinary approach highlights the synergy between microbiology and materials engineering, offering a novel and eco-friendly method for preserving cultural assets.

Marble and limestone have long been used in historical monuments due to their durability and aesthetic value. However, these structures are exposed to environmental stressors and pollutants that gradually degrade the stone.

In the absence of restoration, such deterioration can lead to substantial structural damage (Liu et al. 2011). Marble, primarily composed of calcium carbonate ($CaCO_3$), has low solubility in water but readily reacts with acids generated by acid rain to form soluble salts. This reaction causes material loss, pore formation, surface abrasion, and discoloration (Naidu et al. 2016). Numerous historical buildings have suffered such damage and remain at risk of further deterioration if not properly restored. Although several restoration methods have been developed, traditional techniques still exhibit critical limitations (Liu et al. 2011).

Acrylic and epoxy resins, commonly used for surface coating, can produce incompatible and potentially harmful films. Furthermore, the widespread use of organic solvents contributes to environmental pollution (Down et al. 1996) and poses health risks, while also diminishing the aesthetic quality of stone surfaces. The high cost and limited longevity of these materials have encouraged the search for sustainable alternatives (Luo et al. 2024). In this context, ureolytic bacteria-mediated $CaCO_3$ precipitation has emerged as a promising bio-based repair mechanism. Studies have demonstrated that bacterial facilitation enhances $CaCO_3$ formation, effectively filling cracks and pores, reducing water permeability, and extending structural lifespan (Sumathi et al. 2020; Zhong et al. 2022; Luhar et al. 2022). The goal of such investigations is to employ microbial self-healing processes to restore the physical integrity of structures (Seifan et al. 2016).

Microbially induced carbonate precipitation (MICP) refers to the mineralization process driven by microbial metabolic activity (Ahmad et al. 2024). During MICP, urease-producing bacteria hydrolyze urea to generate carbonate ions (CO_3^{2-}), which react with calcium ions (Ca^{2+}) in the environment to form $CaCO_3$ precipitates (De Muynck et al. 2010; Achal and Pan 2014). The process is influenced by various environmental and biochemical parameters, including pH, temperature, ion concentration, the carbonate-to-calcium ratio, and the presence of additives (Liendo et al. 2022). Among the polymorphs of $CaCO_3$—calcite, aragonite, and vaterite—calcite is the most thermodynamically stable form.

In recent years, increasing attention has been paid to the role of carbon dioxide (CO_2) in enhancing biomineralization efficiency (Isar 2020; Polat 2019). When applied as a surface pre-treatment, CO_2 can modify marble surface chemistry and influence local carbonate equilibria, which in turn promotes more uniform $CaCO_3$ crystal formation. However, excessive CO_2 concentrations or prolonged exposure may drive the system toward high supersaturation, leading to the formation of larger but less adherent crystals (Feng et al. 2007). In addition to gas-related parameters, the calcium source plays a critical role in controlling the morphology and density of precipitated crystals (Anbu et al. 2016).

Calcification can occur through different nucleation pathways, depending on bacterial viability and surface properties, as microbial cell surfaces and extracellular components may serve as nucleation sites for carbonate formation (Keren-Paz et al. 2022; Zhu and Dittrich 2016). In contrast, dead bacterial cells and cellular remnants can promote carbonate precipitation through surface-mediated (passive) nucleation mechanisms, as mineral formation occurs on pre-existing cellular templates in the absence of metabolic activity, although the role of dead cells in biomineralization remains less explored (Robles-Fernández et al. 2022).

The present study investigates the potential of *Bacillus subtilis* ATCC 6633 to repair marble cracks via MICP. *B. subtilis* is a Gram-positive, spore-forming bacterium known for its resilience and environmental adaptability. Owing to its well-characterized genome, it serves as a model organism for studies on bacterial physiology, biofilm formation, quorum sensing, and antibiotic resistance (Su et al. 2020). In this study, both live and dead *B. subtilis* cells were evaluated to determine their respective roles in calcium carbonate precipitation, and the influence of CO_2 pre-treatment on biomineralization efficiency was systematically examined. Controlling CO_2 concentration is thus essential to optimize the microstructure and adhesion of the biogenic calcite layer formed on marble surfaces.

Materials and methods

Chemical materials and marble samples

The chemical reagents used in this study included urea ($CO(NH_2)_2$), yeast extract, D-glucose monohydrate ($C_6H_{12}O_6 \cdot H_2O$), calcium acetate ($(CH_3COO)_2Ca$), calcium chloride dihydrate ($CaCl_2 \cdot 2\ H_2O$), sodium hydroxide (NaOH), physiological saline solution (0.9% NaCl, w/v), and ethyl alcohol (C_2H_5OH).

Marble samples were obtained from a private marble processing company. Square marble specimens measuring 2×2 cm and 4×4 cm were prepared by cutting from larger blocks. For each experimental group, a total of 50 marble samples were used. Prior to experimental treatments, all marble specimens were stored in clean, dry containers under ambient laboratory conditions (Fig. 1).

Microorganism and culture conditions

In this study, *Bacillus subtilis* ATCC 6633, obtained from the American Type Culture Collection (ATCC), was used. The strain was routinely cultured on brain heart infusion



Fig. 1 Representative macroscopic images of untreated marble samples before experimental treatment and bacterial inoculation

agar (BHIA) at 37 °C. Short-term storage of the cultures was carried out at 4 °C until further use.

Preparation of marble samples

Square marble samples measuring 4 × 4 cm were immersed in 70% (v/v) ethanol for 30 min to ensure surface sterilization. During immersion, the samples were rotated at 15-min intervals to allow uniform contact of all surfaces with the alcohol solution. Following sterilization, the marble samples were removed from the solution and dried in an oven at 40 °C for 6 h. During drying, the samples were periodically rotated to ensure complete and uniform drying of all surfaces. After drying, both surfaces of each marble sample were exposed to ultraviolet (UV) radiation for 30 min. The same sterilization and preparation procedures were applied to the 2 × 2 cm marble samples. Following UV treatment, the samples were transferred to sterile containers and stored aseptically until use in subsequent experiments. For surface pre-conditioning, half of the prepared marble samples were placed in a controlled CO_2 chamber maintained at 75% relative humidity and 5% CO_2 for 30 days.

Bacterial inoculation

Prior to bacterial calcification experiments, *Bacillus subtilis* was inoculated into brain heart infusion broth (BHIB) and incubated for 24 h at 37 °C. Subsequently, 0.1 mL of this culture was transferred into 20 mL of fresh BHIB and incubated for an additional 24 h at 37 °C with shaking at 110 rpm. Viable cell counts were determined using the standard plate count method. Serial dilutions of the bacterial culture were prepared in sterile physiological saline solution (0.9% NaCl, w/v). Aliquots of 100 µL from appropriate dilutions were spread evenly onto brain heart infusion agar (BHIA) plates using a sterile L-shaped spreader. The plates were incubated at 37 °C for 24 h, after which colony-forming units (CFU) were counted, and the viable cell concentration of the bacterial culture was calculated.

Preparation of media used in bacterial calcification and sample application

Preparation of the inoculation medium

The inoculation medium consisted of yeast extract (25 g/L) and urea (25 g/L). For experiments involving 4 × 4 cm marble samples, 18 sterile glass jars with a maximum volume of 300 mL were prepared. Similarly, for experiments using 2 × 2 cm marble samples, 18 sterile glass jars with a maximum volume of 100 mL were used. Volumes of 120 mL and 15 mL of inoculation medium were added to the large and small jars, respectively. All media were sterilized by autoclaving at 121 °C for 20 min.

Preparation of the precipitation media

Two different precipitation media were prepared to investigate calcium carbonate formation. The first medium contained calcium acetate [$Ca(CH_3COO)_2$] (6 g/L), glucose (2 g/L), yeast extract (2 g/L), and urea (12 g/L). The second medium consisted of calcium chloride dihydrate ($CaCl_2 \cdot 2\ H_2O$) (60 g/L) and urea (24 g/L). The prepared media were distributed into sterile glass jars of appropriate volumes and sterilized by autoclaving.

Inoculation and experimental groups

The *Bacillus subtilis* liquid culture was inoculated into the inoculation and precipitation media according to the experimental design summarized in Table 1. Experimental groups were categorized as follows: bacteria-free groups (Groups 1, 2, 8, and 9), live-bacteria groups (Groups 3, 4, 10, and 11), and dead-bacteria groups (Groups 5, 6, 12, and 13). Bacteria-free groups served as negative controls, whereas dead-bacteria groups were included to evaluate passive, non-metabolic contributions to calcium carbonate precipitation. Prior to inoculation, bacterial suspensions were adjusted to a final concentration of 10^7 CFU/mL. Cultivation was performed in either small or large glass jars, depending on the marble sample size.

Bacterial coating applications on marbles

For bacterial coating, the inoculation media in large and small jars were inoculated with 100 µL and 10 µL of bacterial suspension, respectively. Inoculation was applied to Groups 3–6 and 10–13, as outlined in Table 1. The jars were covered with sterile sponge plugs to allow gas exchange and incubated at 37 °C with shaking at 90 rpm for 24 h.

Following this incubation period, cultures designated for dead-bacteria treatments were removed from the incubator and autoclaved at 121 °C for 20 min, with jar lids securely closed to prevent liquid loss. Groups without bacterial inoculation were maintained in the dark at room temperature for 24 h under identical conditions.

After preparation of the inoculation media, marble samples were fully immersed to ensure contact of all surfaces with the culture medium. The jars were again covered with sterile sponge plugs, and the marble samples were incubated statically at 28 °C for 2 days to allow bacterial attachment and surface interaction.

Subsequently, the marble samples were aseptically transferred to the corresponding precipitation media. The samples were incubated statically at 28 °C for an additional 4 days, allowing calcium carbonate precipitation to occur on the marble surfaces. After completion of the precipitation stage, the marble samples were incubated at 30 °C for 2 days and then stored at 24 °C under air-conditioned laboratory conditions for 3 months to allow crystal maturation and stabilization. Marble samples subjected to CO_2 pre-treatment were processed using the same post-precipitation incubation protocol. All control groups were maintained under identical conditions throughout the experiment.

Table 1 Composition of media and experimental grouping used in biocalcification assays

CO_2Condition	Inoculation Medium	Bacteria Application	Precipitation Media	Group #
CO_2 pre-treated	YEU[a]	None	CaAcetatGYE[b]+U[c]	1
			$CaCl_2$+U	2
		Live	CaAcetatGYE+U	3
			$CaCl_2$+U	4
		Dead	CaAcetatGYE+U	5
			$CaCl_2$+U	6
	—	None	—	7 (Control)
CO_2 untreated	YEU	None	CaAcetatGYE+U	8
			$CaCl_2$+U	9
		Live	CaAcetatGYE+U	10
			$CaCl_2$+U	11
		Dead	CaAcetatGYE+U	12
			$CaCl_2$+U	13
	—	None	—	14 (Control)

[a]YEU: Yeast extract-urea medium

[b]CaAcetatGYE: Medium containing $Ca(C_2H_3O_2)_2$, glucose and yeast extract

[c] U: Urea

None: Bacteria-free

"—": No inoculation or precipitation medium applied

Instrumental analysis

X-ray diffraction (XRD)

The crystal structure of the identification powdered marble samples were analyzed by XRD. Rigaku Rad B-Dmax II powder X-ray diffraction meter was used. Changed the value of 2θ by 20° to 80° with 0.04° step size using Cu Kα radiation. 5 mg samples were on a coverslip with silica grease.

Scanning electron microscopy (SEM) combined with energy dispersive x-ray analysis (EDX) (SEM-EDX)

The surface morphology of the marble samples was displayed using SEM (LEO Evo-40 VPX microscope). Chemical composition analysis was performed with EDX, using Rönteck xflash detector analyzer associated with Scanning electron microscope (SEM, Leo-Evo 40xVP).

Atomic force microscopy (AFM)

Atomic force microscopy (AFM; XE-100E, Park Systems Corp., Suwon, Korea) was employed to quantitatively evaluate surface topography and pore/crack geometry of

the marble samples. The maximum pore (or crack) depth was defined as the vertical height difference between the bottom of surface pores or cracks and the adjacent intact marble surface. This parameter was determined from AFM height images using line profile analysis across representative pores and cracks. Measurements were performed at four different regions per sample, and results are reported as mean ± standard deviation. Although AFM line profile analysis involves measuring vertical height differences, the measurements in this study were performed specifically across individual pores and cracks to determine their depth, rather than using peak-to-valley values to describe overall surface roughness.

Pore size was defined as the lateral pore dimension measured from stereomicroscopic and SEM images, and pores were classified as micropores or macropores based on their measured size ranges.

Results

Macroscopic and stereomicroscopic imaging results

Following the completion of a three-month incubation period, macroscopic examination of the surfaces of the 4 × 4 cm marble samples revealed the presence of white, fine granular deposits localized within the inner regions of the macropores in samples from the CO_2-pre-treated group containing live bacteria (Group 4). These deposits appeared as discrete accumulations within pore structures rather than as continuous surface layers.

Stereomicroscopic observations further confirmed the presence of calcium carbonate deposits in Group 4 samples. In contrast, no $CaCO_3$ crystal formation was detected on the marble surfaces of the CO_2-pre-treated control group (Group 7), the CO_2-untreated control group (Group 14), or the bacteria-free groups (Groups 1, 2, 8, and 9). Similarly, marble samples that were not subjected to CO_2 pre-treatment did not exhibit detectable $CaCO_3$ deposition, regardless of whether live or dead bacteria were present.

As shown in Fig. 2b and c, the macropores of marble samples treated with live bacteria in calcium chloride medium exhibited partial closure, whereas the micropores were largely filled as a result of $CaCO_3$ precipitation. Microscopic observations revealed that the newly formed mineral structures were clearly distinguishable from the original marble matrix and were associated with pores exhibiting pore sizes in the range of approximately 3–5 mm. Calcium carbonate deposition on the marble surfaces was more pronounced in the calcium chloride–containing medium than in the calcium acetate medium. In addition, the morphology of the precipitated $CaCO_3$ differed between the two media: in the $CaCl_2 \cdot 2\ H_2O$ medium, granular white crystalline deposits were observed (Fig. 3), whereas in the $Ca(CH_3COO)_2$-containing medium, the deposits appeared as fine, powdery layers.

Figure 2 $CaCO_3$ crystals formed on CO_2-pre-treated marble surfaces in $CaCl_2$+U medium (10× magnification): (a) control group (Group 7); (b) live-bacteria-treated group (Group 4); (c) dead-bacteria-treated group (Group 6).

Microscopic examination showed that marble samples treated with live bacteria in calcium chloride medium developed less complex surface structures than those observed in CO_2-pre-treated samples. Stereomicroscopic observations revealed no detectable crystal formation in samples containing dead bacteria or in samples that were not subjected to CO_2 pre-treatment. In contrast, SEM analysis revealed the presence of $CaCO_3$ crystal structures in both live- and dead-bacteria-treated samples, although crystal abundance and surface coverage were markedly lower in the CO_2-untreated groups. Furthermore, surface coverage and macropore filling were less extensive in the CO_2-untreated samples than in the CO_2-pre-treated samples.

Microscopic examination showed that the surface structures formed on marble samples treated with live bacteria in a calcium chloride medium were less complex than those observed in comparable samples subjected to CO_2 pre-treatment. Stereomicroscopic observations revealed no detectable crystal formation in samples containing dead bacteria or in samples that were not subjected to CO_2 pre-treatment. In contrast, SEM analysis revealed the presence of $CaCO_3$ crystal structures in both live- and dead-bacteria-treated samples, although crystal abundance and surface coverage were markedly lower in the CO_2-untreated groups. Furthermore, surface coverage and macropore filling were less extensive in the CO_2-untreated samples than in the CO_2-pre-treated samples.

Effects of Live/Dead Cells, culture Media, and CO_2 Pre-treatment on biocalcification efficiency

Comparative evaluation of the marble samples demonstrated that biocalcification efficiency was strongly influenced by bacterial viability (live versus dead cells), the type of culture medium, and CO_2 pre-treatment. These factors governed not only the extent of $CaCO_3$ deposition but also the resulting crystal polymorphs (calcite, aragonite, and vaterite) and the spatial distribution of precipitates within marble pores. SEM observations revealed distinct $CaCO_3$ crystal structures within the micropores of treated marble samples, which were distinguishable from the original marble matrix based on their morphology and size. In contrast, the marble surfaces of the control group retained their

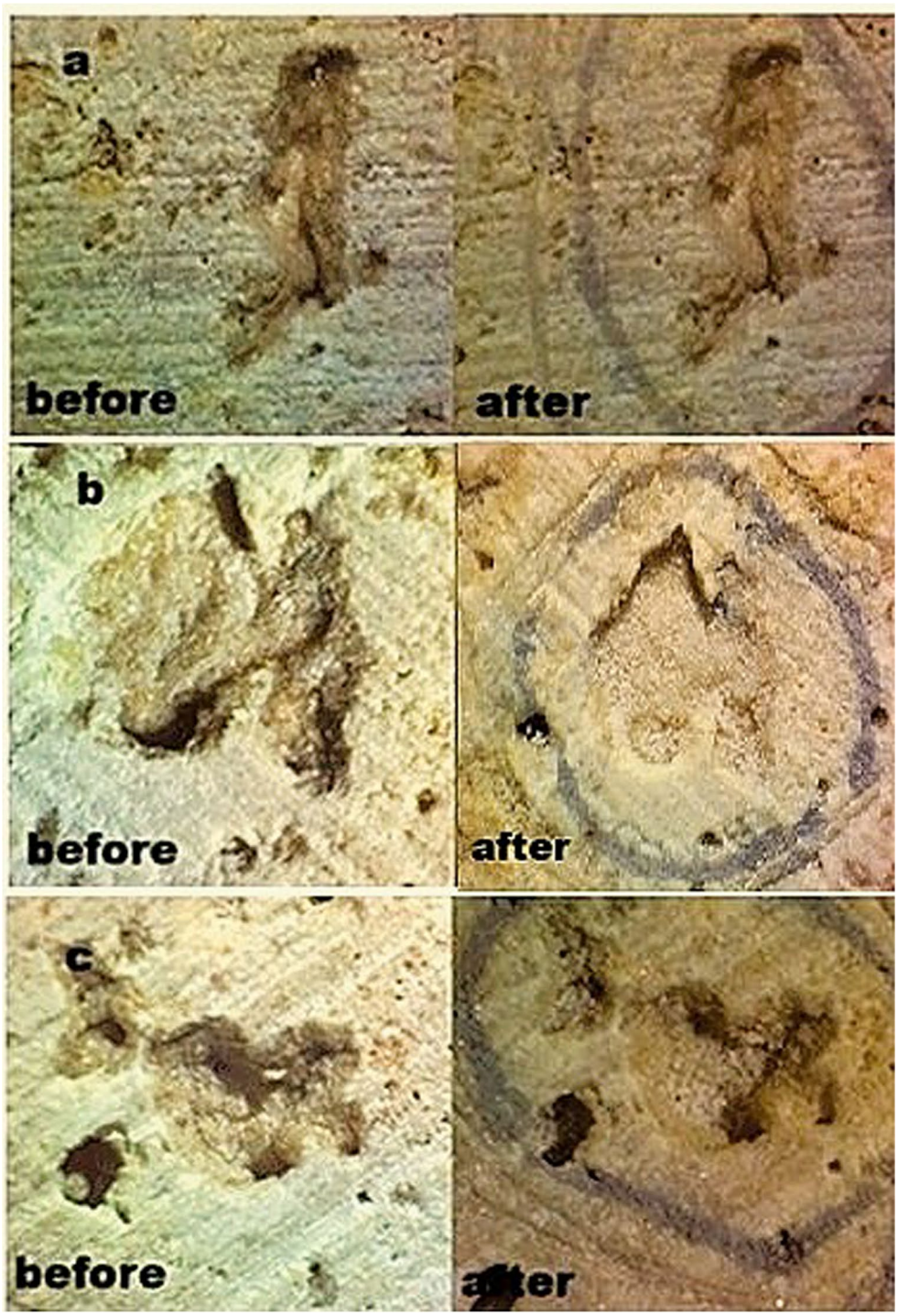

Fig. 2 $CaCO_3$ crystals formed on CO_2-pre-treated marble surfaces in $CaCl_2$+U medium (10× magnification): (**a**) control group (group 7); (**b**) live-bacteria-treated group (group 4); (**c**) dead-bacteria-treated group (group 6)

original amorphous appearance, with no evidence of crystal formation (Fig. 4).

These findings were further supported by SEM imaging, which provided clear evidence of bacterial calcification. SEM images revealed calcite and aragonite crystals with sizes ranging from approximately 20 to 100 µm on the marble surfaces and within micropores. The biogenic $CaCO_3$ deposits partially filled pore spaces and were distinguishable from the amorphous surface structures observed in the control group. Among all experimental groups, Group 4 exhibited the most extensive biocalcification, characterized by the largest and densest crystal formations (Fig. 5).

Beyond morphological observations, SEM-EDX and elemental mapping analyses provided chemical support for bacterial calcification. Figures 6 and 7 present SEM-EDX

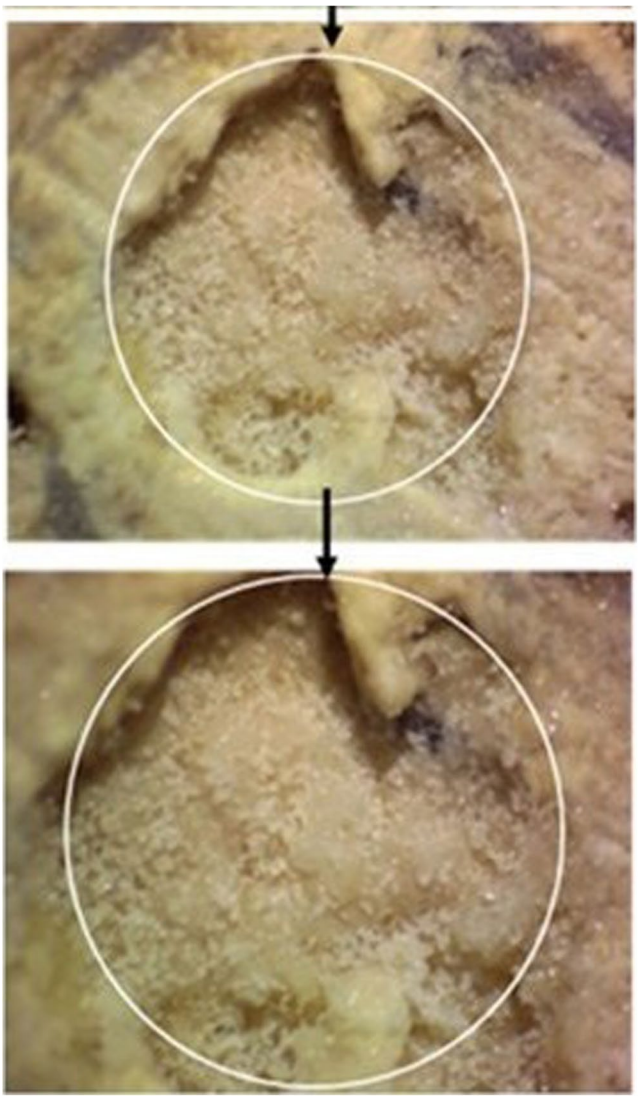

Fig. 3 Stereo microscopic images of $CaCO_3$ crystals formed by live bacteria on CO_2-pre-treated marble surfaces incubated in $CaCl_2$+U medium (group 4) at 10x and 15x magnification

spectra and elemental mapping analyses of marble surfaces from the CO_2-pre-treated control group and Group 4. EDX analysis showed that the carbon content of CO_2-pre-treated marble samples was higher than that of untreated control samples. Furthermore, SEM-EDX results indicated that the newly formed structures associated with bacterial calcification exhibited elevated Ca, C, and O signals compared to the control group, consistent with the presence of calcium carbonate (Fig. 7).

In addition, EDX spectra confirmed the elemental composition of the marble, showing prominent signals corresponding to calcium (Ca), carbon (C), silicon (Si), and oxygen (O). Compared to the control group, bacteria-treated and nutrient-supplemented samples exhibited higher relative Ca signals, while O and Si signals were comparatively reduced.

Quantitative EDX analysis revealed that marble samples treated with live bacteria in CaU medium (Group 4) displayed the highest calcium content (48.88%; Fig. 7), whereas the control group lacking both bacterial activity and nutrient supplementation exhibited a lower calcium content (34.95%; Fig. 6). These compositional differences are consistent with enhanced calcium carbonate deposition in the biocalcified samples.

The production of calcium carbonate crystals by living bacteria was supported by the presence of characteristic elemental peaks detected in the EDX spectra. Additional evidence was obtained from analyses of material scraped from distinct crystalline structures observed within the macropores of the 4 × 4 cm marble surfaces in Group 4. SEM-EDX analysis of these scraped samples confirmed their calcium carbonate composition (Fig. 8).

In addition, SEM-EDX and elemental mapping analyses were performed on the scraped samples. These analyses identified the presence of calcite and aragonite crystal phases within the sampled material. Quantitative EDX analysis indicated a calcium content of 43.46% in these samples (Fig. 9). The corresponding EDX spectra displayed characteristic elemental peaks consistent with calcium carbonate composition.

Following the analysis of live-cell treatments, the effects of dead bacterial cells on biocalcification were also examined. SEM analysis of CO_2-pre-treated marble surfaces treated with dead bacteria and immersed in $CaCl_2$+U medium (Group 6) revealed the presence of calcite, aragonite, and amorphous phases (Fig. 10). Calcium carbonate crystals were observed on the marble surfaces in the dead-cell-treated samples; however, crystal density was markedly lower than that observed in samples treated with live cells under the same conditions. Consistent with these observations, SEM-EDX analysis showed that the Ca content in dead-cell-treated groups was higher than in the control group but lower than in the corresponding live-cell-treated groups (data not shown).

Given the influence of nutrient composition and calcium source on biocalcification, an alternative medium (CaAcetatGYE+U) was also evaluated. In contrast to the more pronounced calcification observed in the $CaCl_2$+U medium, Groups 3 and 5 maintained in CaAcetatGYE+U exhibited sparse, low-density aragonite and vaterite deposits in SEM analyses. These deposits were limited in extent, suggesting that micropore filling was less developed under these conditions (Fig. 11).

To assess the effect of CO_2 pre-treatment on biocalcification, CO_2-untreated marble samples were also examined. Macroscopic, stereomicroscopic, and SEM analyses of CO_2-untreated samples inoculated with live bacteria in $CaCl_2$+U medium revealed no detectable $CaCO_3$ polymorphs. In contrast, SEM images of CO_2-untreated samples treated with dead bacteria showed the presence of sparse, needle-like

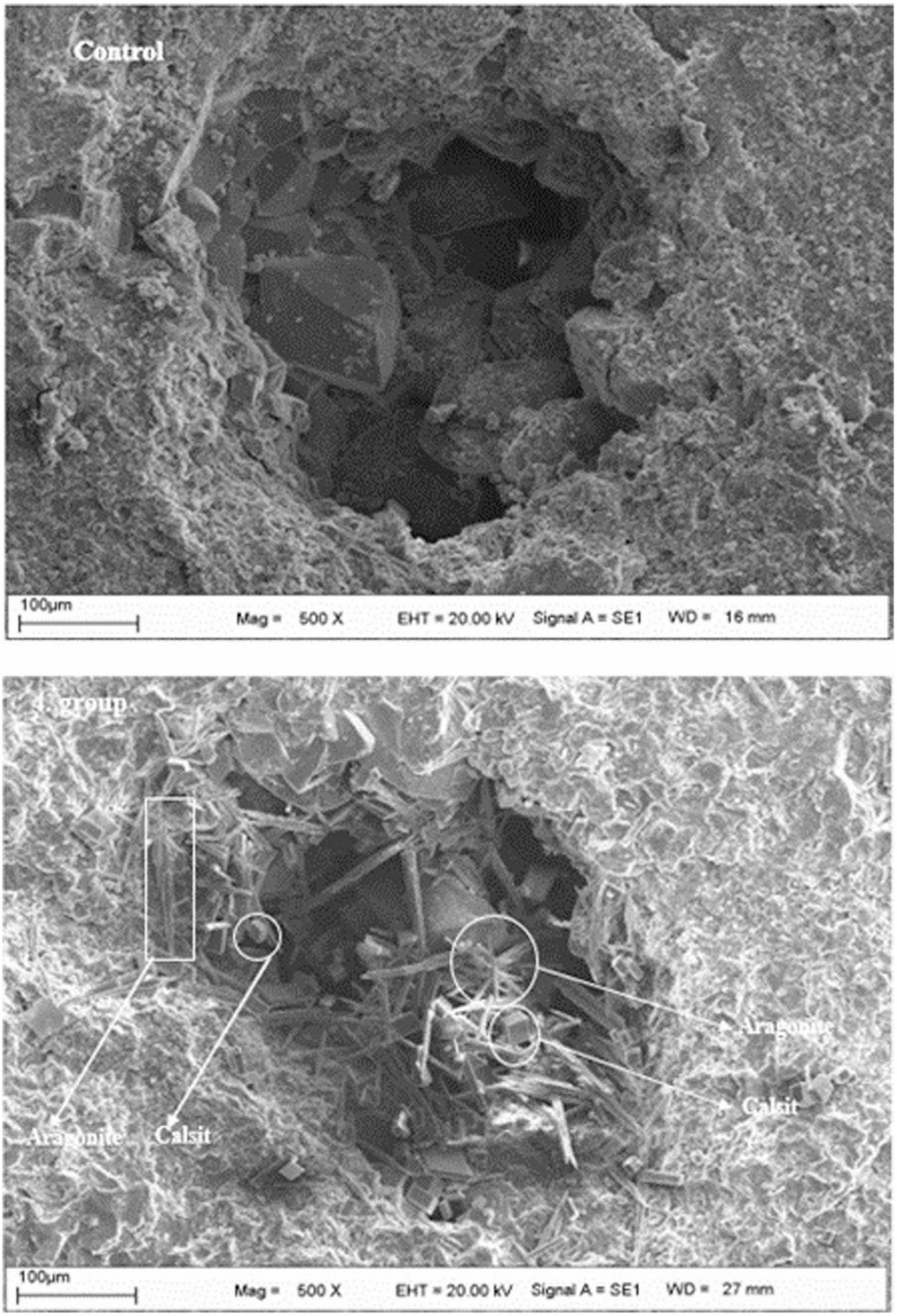

Fig. 4 SEM images of CO_2-pre-treated marble surfaces from the control group and $CaCO_3$ crystals formed by live bacteria on CO_2-pre-treated marble surfaces incubated in $CaCl_2$+U medium (group 4)

aragonite structures with average lengths of approximately 20 µm, although their density was lower than that observed in live-bacteria-treated samples under CO_2-pre-treated conditions (Fig. 12).

SEM-EDX analysis further indicated lower carbon levels in the CO_2-untreated control samples compared to the CO_2-pre-treated controls (data not shown). Similarly, no $CaCO_3$ crystals were detected in CO_2-untreated samples maintained in CaAcetateGYE medium with live bacteria; instead, predominantly amorphous surface structures resembling the native marble matrix were observed. Overall, these observations indicate that CO_2 pre-treatment is associated with enhanced $CaCO_3$ formation and more pronounced differences between live- and dead-bacteria-treated samples.

SEM analysis of CO_2-untreated marble surfaces treated with dead bacteria revealed the presence of vaterite as

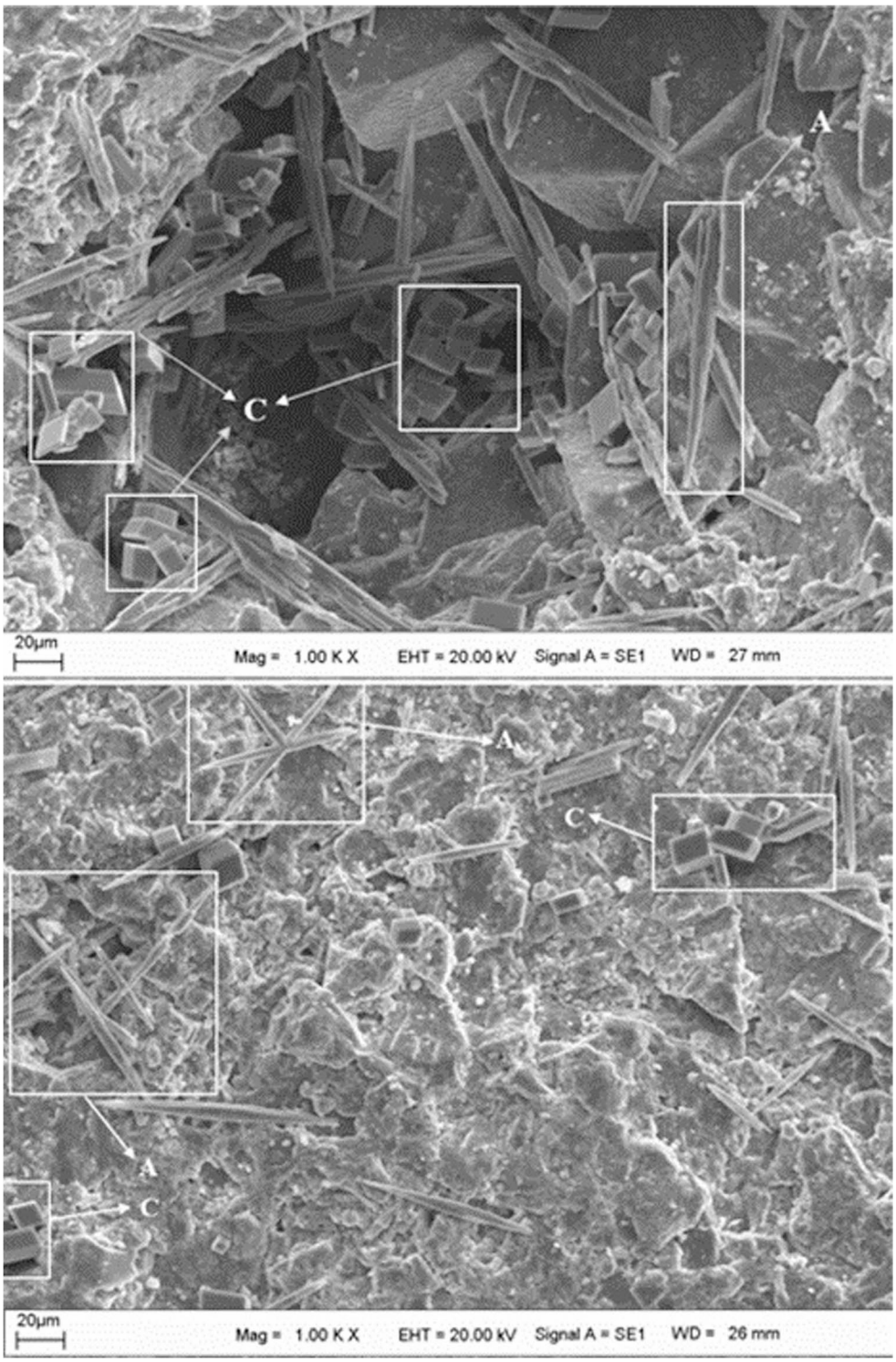

Fig. 5 SEM images of $CaCO_3$ crystals formed by live bacteria on CO_2-pre-treated marble surfaces incubated in $CaCl_2$+U medium (group 4). C, calcite; A, aragonite

the dominant calcium carbonate polymorph (Fig. 13). In contrast, SEM examination of CO_2-untreated and bacteria-free marble surfaces maintained in $CaCl_2$+U medium showed only limited crystal formation, with the detected $CaCO_3$ polymorphs predominantly corresponding to aragonite (Fig. 14).

As summarized in Table 2, the combination of CO_2 pre-treatment and live bacterial application was associated with the most extensive biohealing features observed on marble surfaces. In this group, crystal sizes ranged from approximately 20 to 100 µm and consisted predominantly of calcite and aragonite. The affected regions were widespread, with both

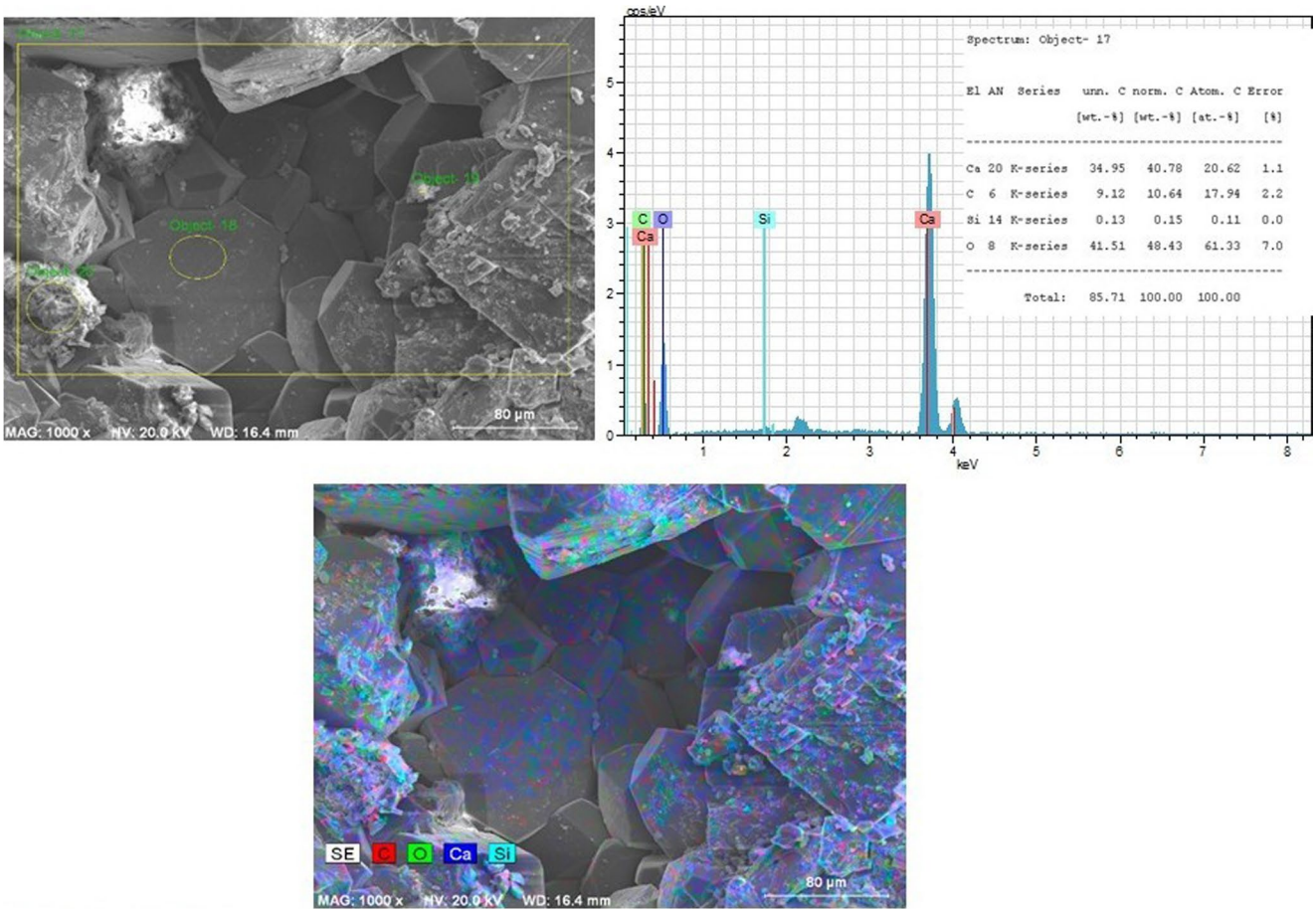

Fig. 6 SEM-EDX and elemental mapping of CO_2-pre-treated marble surfaces from the control group (group 7)

micro- and macropores partially or fully filled, as reflected by measured pore diameters of 0.214 mm and 0.059 mm, pore areas of 0.033 × 0.062 mm² and 0.031 × 0.066 mm², and macropores of approximately 3 × 5 mm exhibiting $CaCO_3$ sealing.

In contrast, CO_2-untreated samples treated with live bacteria exhibited only smaller aragonite crystals (10–20 µm), and no measurable biohealed areas were detected. Samples treated with dead bacteria showed limited calcification. Under CO_2-pre-treated conditions, crystals with sizes of 10–20 µm (calcite and aragonite) were observed, whereas the biohealed area was restricted to a diameter of approximately 0.036 mm. In the absence of CO_2 pre-treatment, crystal sizes were further reduced (1–10 µm) and were predominantly composed of vaterite. Overall, the data in Table 2 illustrate clear differences in crystal size, polymorph distribution, and pore filling across the experimental groups.

XRD analysis results

The XRD diffractogram presented in Fig. 15 corresponds to calcium carbonate crystals extracted from the macropores of CO_2-pre-treated marble surfaces incubated in $CaCl_2$+U medium (Group 4). The diffraction pattern was consistent with well-crystallized calcite ($CaCO_3$), as evidenced by the dominant reflection at approximately 29.4° 2θ corresponding to the (104) plane. Additional characteristic calcite reflections were observed at 23.1°, 36.0°, 39.4°, 43.1°, 47.5–48.5°, 57.5°, 60.7–61.0°, and 65.3° 2θ, in good agreement with standard calcite reference data (Table 3). Calcite was identified as the dominant crystalline phase in the XRD patterns.

AFM analysis results

AFM analysis revealed distinct differences in surface topography and pore/crack geometry between control and biocalcified marble samples. The maximum pore (or crack) depth, determined from AFM height images using line profile analysis, decreased from 35.00 ± 7.07 µm in the control group to 22.50 ± 8.20 µm in biocalcified samples (Fig. 16). This reduction reflects partial filling of surface pores and cracks and a smoother surface morphology associated with $CaCO_3$ deposition induced by microbial activity.

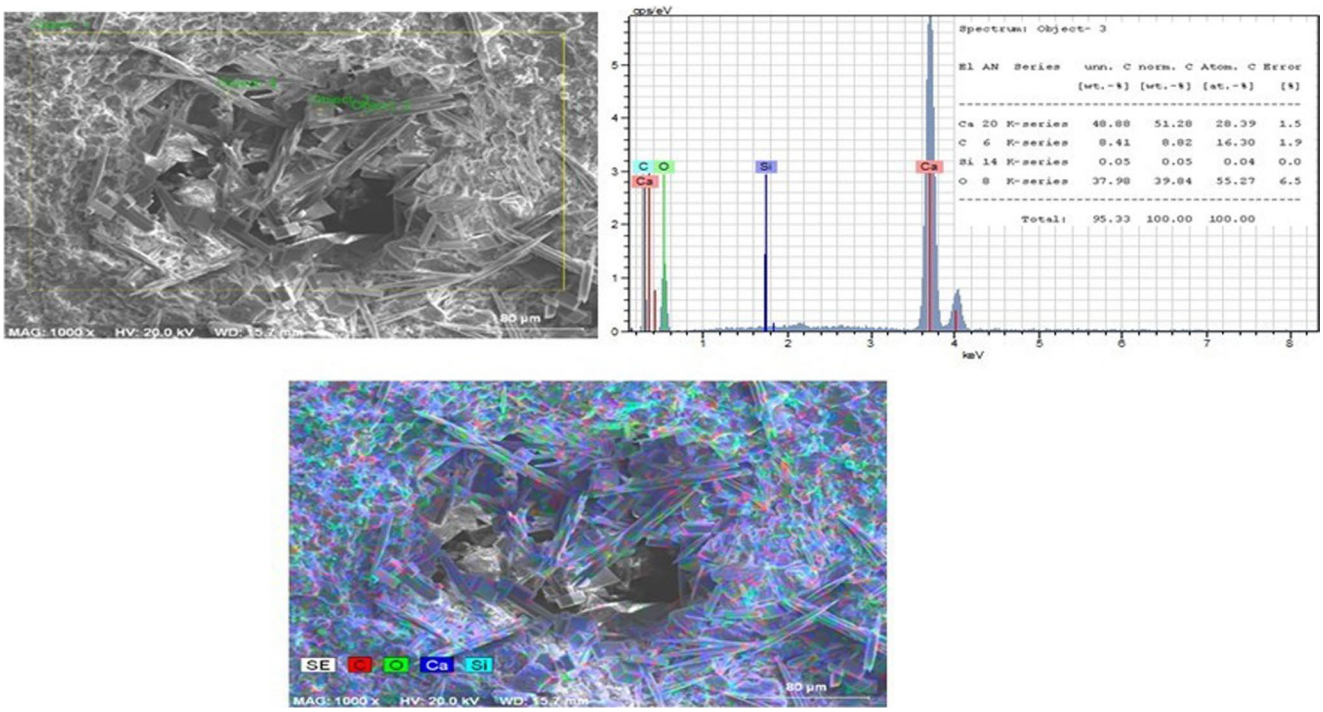

Fig. 7 SEM-EDX and elemental mapping of $CaCO_3$ crystals formed by live bacteria on CO_2-pre-treated marble surfaces incubated in $CaCl_2$+U medium (Group 4)

The effect of CO_2 pre-treatment on marble surface chemistry was further supported by microstructural and compositional analyses. SEM-EDX and elemental mapping (Figs. 6 and 7) revealed an increased carbon signal on CO_2-pre-treated marble surfaces compared to untreated controls, indicating enhanced surface carbon availability following CO_2 exposure under humid conditions. This chemical preconditioning promoted Ca^{2+}–CO_3^{2-} supersaturation at the surface, facilitating nucleation and growth of $CaCO_3$ crystals during microbial activity. Consistently, XRD analysis of crystals extracted from CO_2-pre-treated samples (Fig. 15) confirmed the formation of well-crystallized calcite, demonstrating that CO_2 pre-treatment played a critical role in stabilizing carbonate mineral phases and enhancing biocalcification efficiency.

Discussion

The present study shows that microbially induced carbonate precipitation (MICP) mediated by *Bacillus subtilis* ATCC 6633 can contribute to the biohealing of marble surfaces by promoting calcium carbonate deposition within surface pores and cracks. The results indicate that bacterial viability and calcium source play key roles in influencing $CaCO_3$ polymorphism and surface modification. Live bacterial cells favored the formation of thermodynamically stable calcite and aragonite phases, whereas dead cells and calcium acetate predominantly resulted in metastable vaterite formation, suggesting different nucleation pathways under biologically active and passive conditions. Furthermore, CO_2 pre-treatment acted as a surface-conditioning step that enhanced inorganic carbon availability and promoted more uniform $CaCO_3$ nucleation, thereby improving biocalcification efficiency. Taken together, these findings support a mechanistic interpretation linking microbial activity, calcium chemistry, and surface preconditioning to marble biohealing. These observations are consistent with established mechanisms governing microbially induced carbonate precipitation and $CaCO_3$ polymorphism.

Microbially induced carbonate precipitation (MICP) is a mineralization process driven by the metabolic activities of microorganisms. Ureolytic bacterial strains hydrolyze urea via the enzyme urease, generating carbonate species that subsequently react with calcium ions to form calcium carbonate. In addition to urease activity, enzymes such as carbonic anhydrase may also contribute to carbonate generation, and the overall precipitation process is governed by a series of interconnected biochemical reactions (Achal and Pan 2014; Alvarado-Mata et al. 2025). Briefly, urea hydrolysis produces ammonia and carbamate, which further decompose into ammonia and carbonic acid. These products interact in aqueous solution to yield ammonium, hydroxide, and bicarbonate ions, leading to an increase in pH. As a result, bicarbonate ions are converted into carbonate ions,

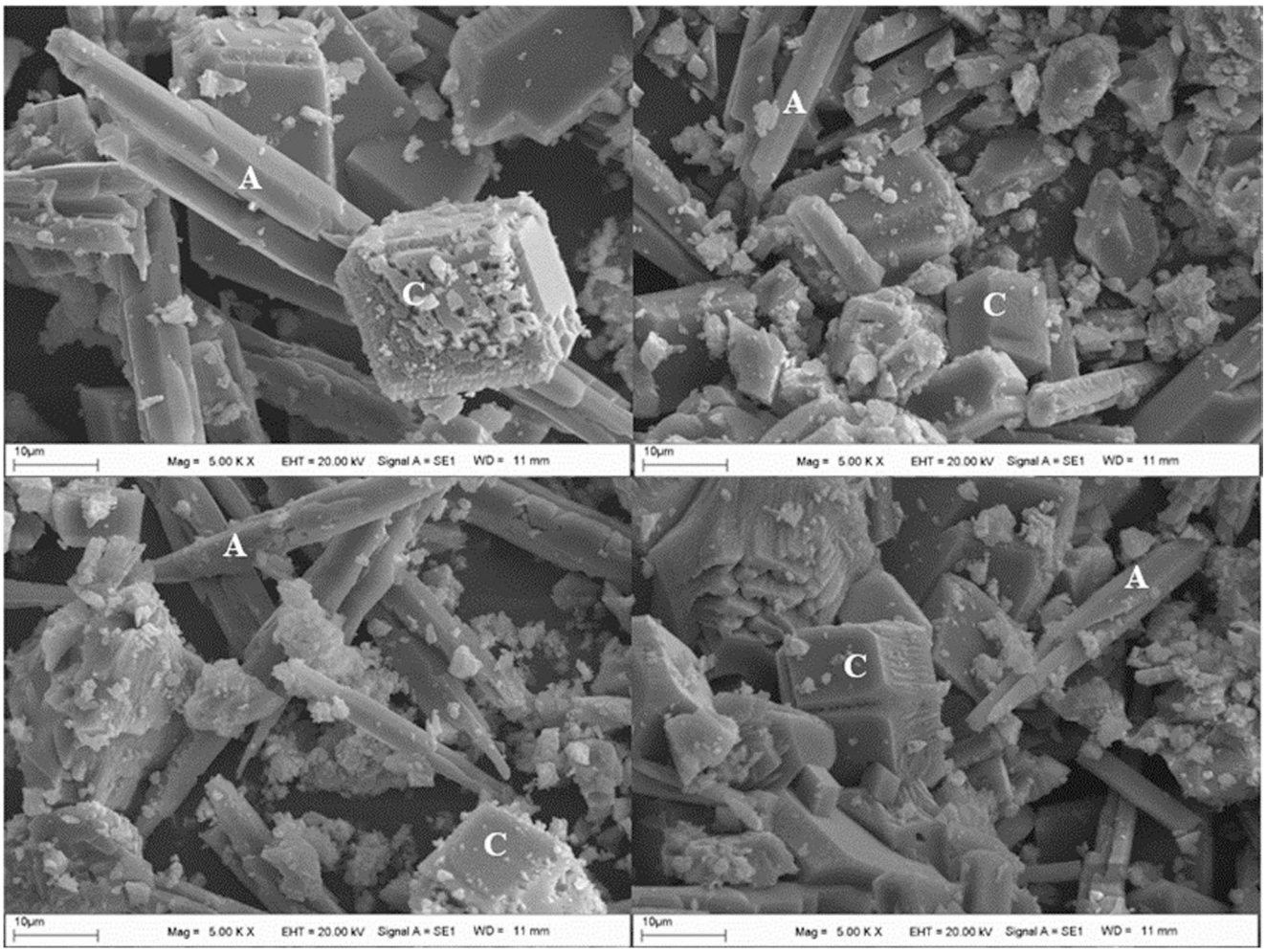

Fig. 8 SEM images of $CaCO_3$ crystals scraped from macropores of CO_2-pre-treated marble surfaces incubated in $CaCl_2$+U medium (group 4, live bacteria) at 5000x magnification. C, calcite; A, aragonite

enabling $CaCO_3$ precipitation in the presence of calcium ions (Hammes et al. 2003).

Bacterial calcium carbonate precipitation can result in the formation of different crystal polymorphs, most commonly calcite, aragonite, and vaterite. Among these, vaterite is a metastable phase that is frequently produced during the early stages of bacterial mineralization and may subsequently transform into the more thermodynamically stable calcite form (Tourney and Ngwenya 2009; Wang and Becker 2009; Bozbeyoğlu et al. 2020; Qafoku et al. 2022). Stereomicroscopic observations of marble macropores at 20× magnification revealed $CaCO_3$ structures consistent with those reported in previous studies (Wiktor and Jonkers 2011). Correspondingly, SEM analyses confirmed the presence of crystalline deposits whose morphology was comparable to that of $CaCO_3$ crystals described in the literature. These biogenic mineral phases were clearly distinguishable from the amorphous marble matrix based on their size, morphology, and visual appearance. In contrast, control marble surfaces exhibited no crystalline deposits and were consistent with previously reported observations for untreated marble materials (Colao et al. 2004; Moropoulou et al. 2019).

B. subtilis has been reported to promote calcite formation in vitro when cultured in media containing different calcium sources, including calcium lactate, calcium acetate, and calcium chloride (Shirakawa et al. 2015). Several Bacillus strains are known to mineralize $CaCO_3$ into distinct polymorphs, most commonly calcite and vaterite (Seifan et al. 2016), although the factors governing polymorph selection remain incompletely understood. In the present study, in addition to calcite, a limited number of aragonite crystals were also identified. Comparable observations have been reported for *Sporosarcina pasteurii*, in which calcite formation was dominant in calcium chloride media, whereas SEM analyses revealed vaterite structures in media containing calcium lactate, calcium acetate, or calcium gluconate (Gorospe et al. 2013). Polymorph transitions are influenced by incubation conditions such as temperature and time, and

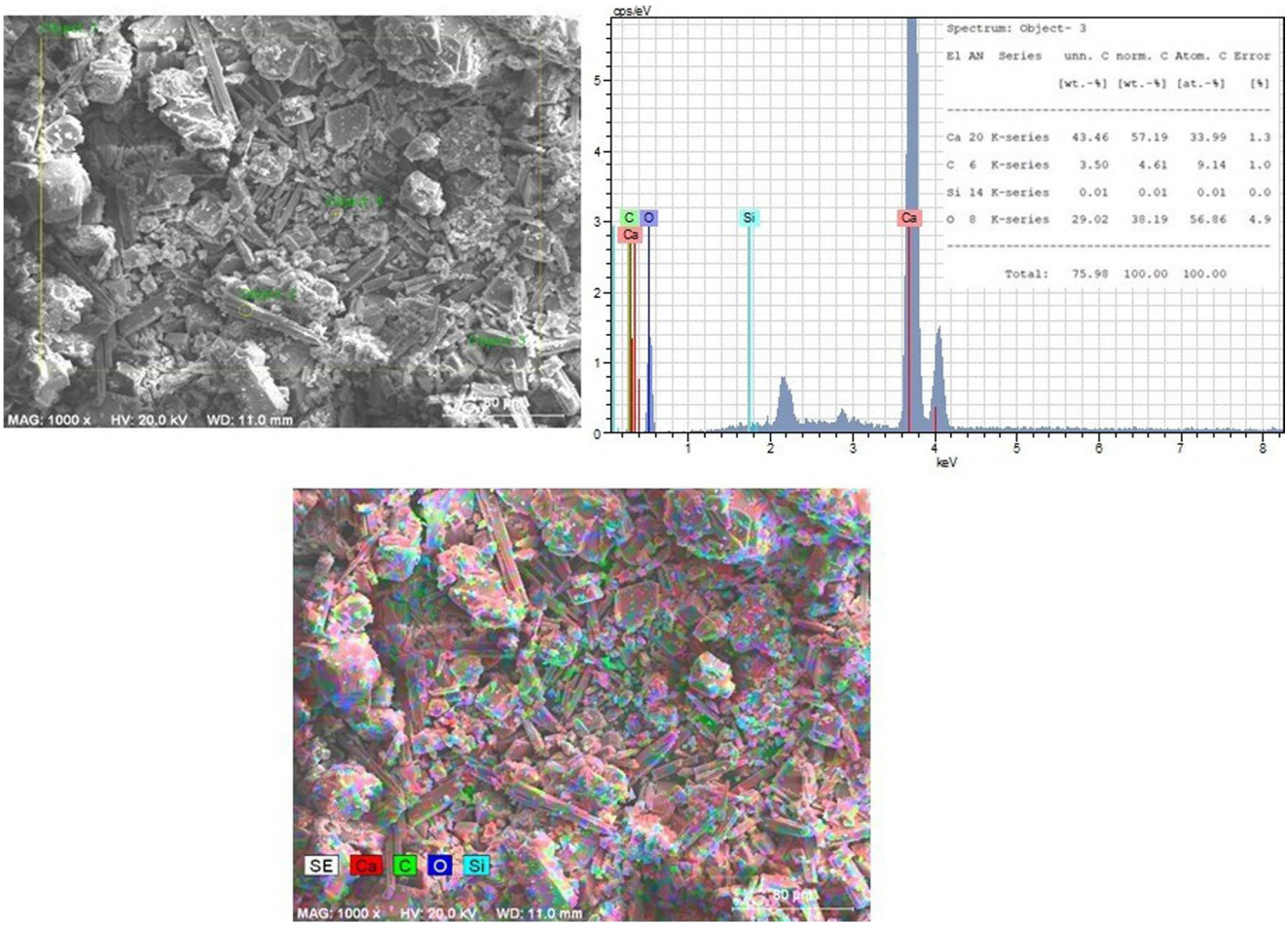

Fig. 9 SEM-EDX and elemental mapping of $CaCO_3$ crystals scraped from macropores of CO_2-pre-treated marble surfaces incubated in $CaCl_2$+U medium (Group 4)

less stable phases such as aragonite may nucleate during early stages of mineralization before gradually transforming into the thermodynamically stable calcite phase (Ramakrishna et al. 2016).

Microorganisms possessing negatively charged cell surfaces and urease activity can hydrolyze urea to generate carbonate species and ammonium, thereby facilitating the binding of calcium ions to the cell surface and inducing $CaCO_3$ precipitation (De Muynck et al. 2010). Under conditions of elevated urea availability, this process is further enhanced, which explains why ureolytic bacteria are commonly selected for MICP applications due to their robustness and adaptability to environmental conditions. Calcium carbonate precipitation typically proceeds through heterogeneous nucleation on the bacterial cell wall once supersaturation is achieved (Siddique and Chahal 2011). For extracellular $CaCO_3$ precipitation to occur via urease- and carbonic anhydrase–mediated reactions, calcium ions must be present at sufficient concentrations. Consequently, both the type and concentration of the calcium source represent critical factors governing the extent and polymorphic outcome of mineralization (Kart 2021). In agreement with this, the present study showed that different calcium sources resulted in distinct $CaCO_3$ polymorphs, with calcium chloride favoring the formation of calcite and aragonite, whereas calcium acetate predominantly promoted vaterite formation.

Vaterite nanoparticles have been reported to exhibit advantageous properties as filler materials, including enhanced hydration kinetics, improved pore filling, and increased mechanical performance in cement-based systems (Li et al. 2024). Similarly, Hargis et al. (2014) demonstrated that vaterite reduced setting time compared to calcite, despite differences in particle size. Although vaterite is a metastable and relatively uncommon $CaCO_3$ polymorph, it can be induced under specific conditions, including biocalcification processes (Mann 2001). The morphology of vaterite is strongly influenced by the calcium source, with calcium acetate promoting lettuce-like lamellar structures, whereas calcium lactate and calcium gluconate favor spherical morphologies (Tai and Chen 1998). In this context, the

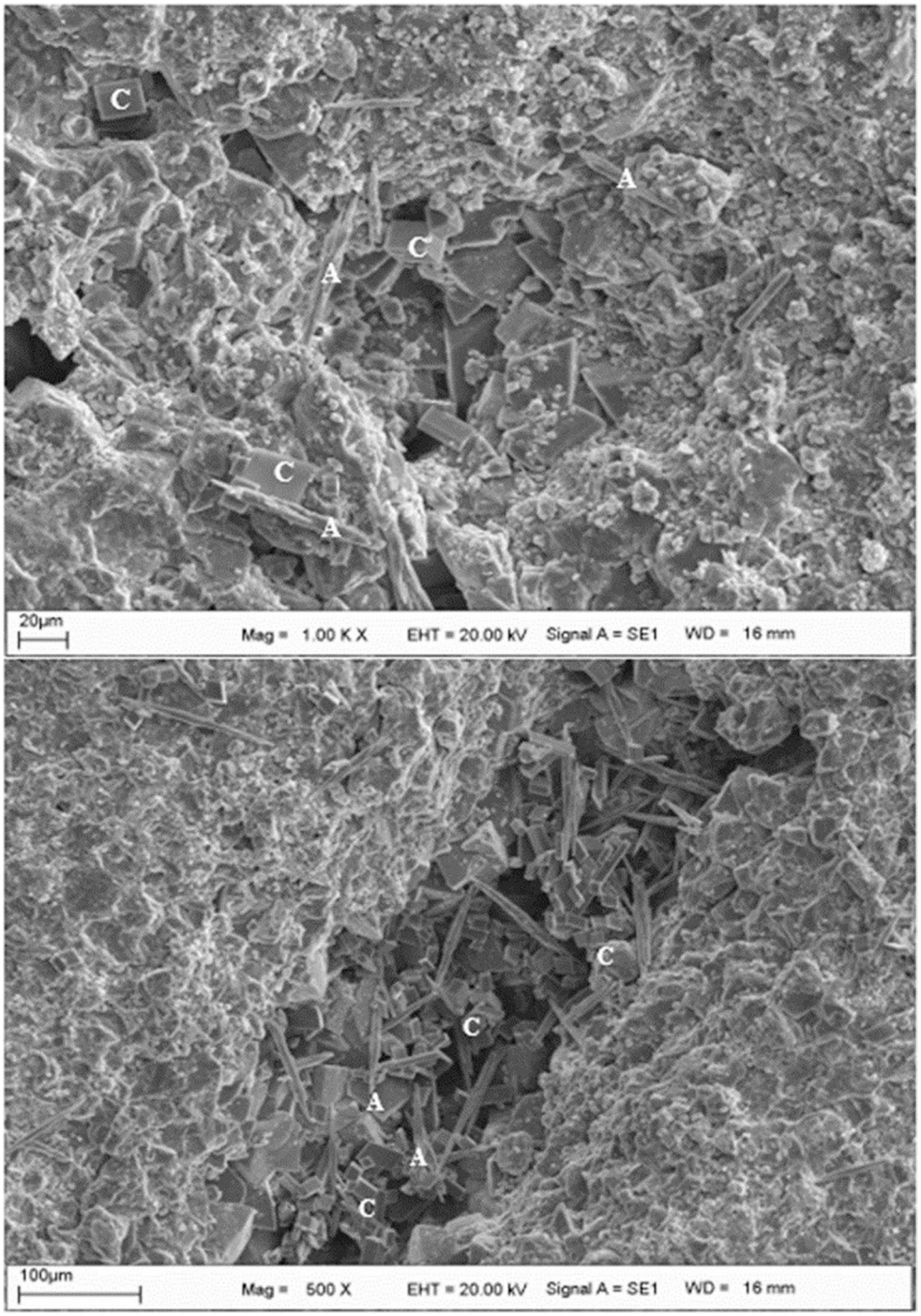

Fig. 10 SEM images of $CaCO_3$ crystals formed on CO_2-pre-treated marble surfaces treated with dead bacteria in $CaCl_2$+U medium (Group 6)

present study highlights the formation of spherical vaterite associated with dead *B. subtilis* cells under calcium-rich conditions, which differs from morphologies commonly reported in the existing literature.

XRD, SEM, and FTIR analyses of *Bacillus sp.* CR2 cultures revealed that calcite was the dominant $CaCO_3$ polymorph, irrespective of whether calcium chloride, calcium oxide, calcium acetate, or calcium nitrate was used as the calcium source. Notably, in calcium acetate–containing media, minor amounts of vaterite and aragonite were also detected (Achal and Pan 2014). Consistent with these observations, a parallel study on biogenic plaster samples prepared using *Sporosarcina pasteurii* ATCC 6453 demonstrated that calcium nitrate– and calcium chloride–treated systems predominantly yielded calcite, whereas calcium acetate–based systems additionally exhibited aragonite and vaterite phases (Zhang et al. 2014).

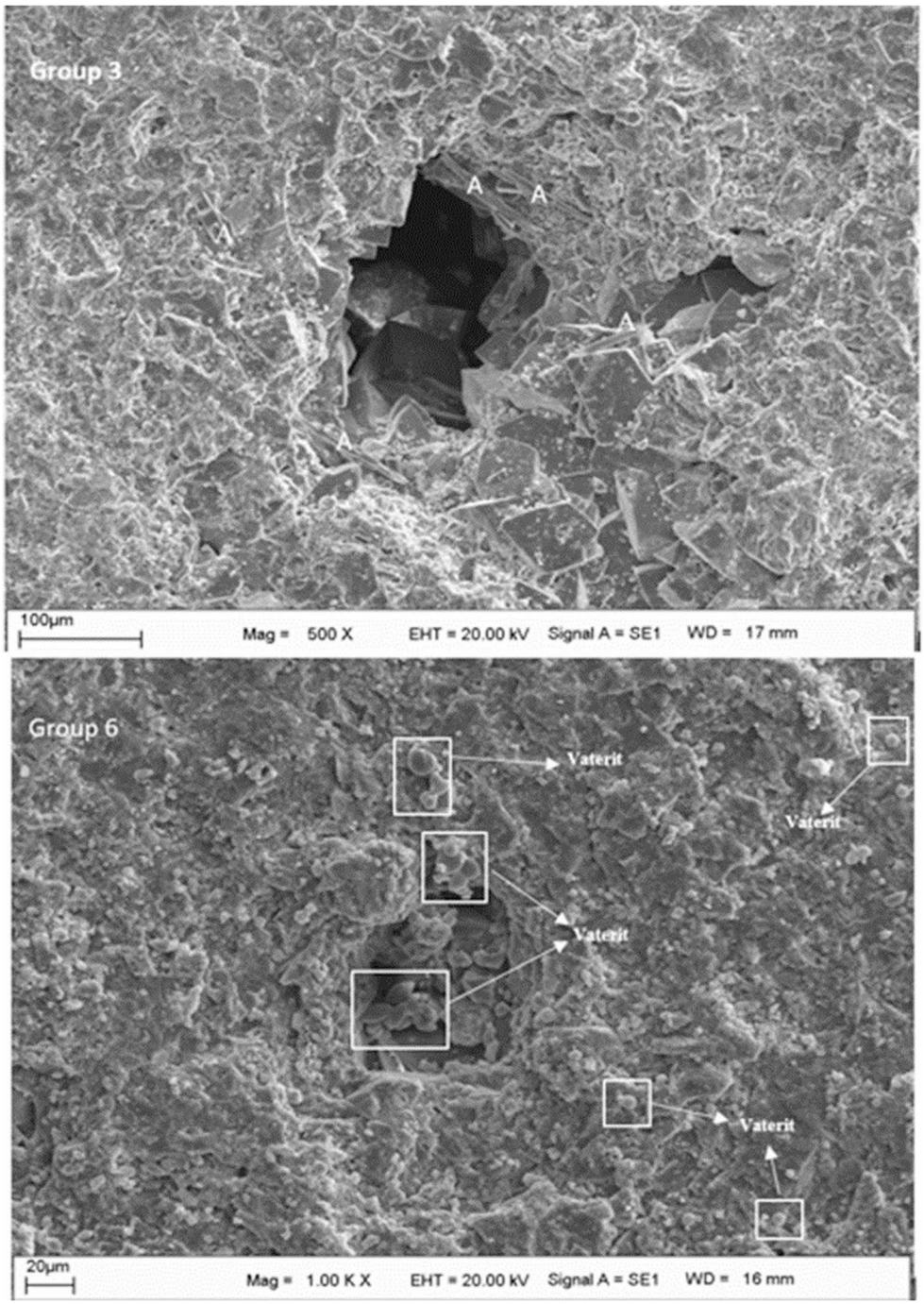

Fig. 11 SEM images of $CaCO_3$ crystals formed on marble surfaces treated with live (group 3, top) and dead (group 5, bottom) bacteria and incubated in CaAcetate-GYE + U medium. V, vaterite

Bacterial carbonate precipitation can occur through both passive and active nucleation (Schultze-Lam and Beveridge 1994; Schultze-Lam et al. 1996; Stocks-Fischer et al. 1999; Warren et al. 2001; Raza and Khushnood 2022). Passive nucleation is primarily driven by metabolically induced changes in the microenvironment surrounding bacterial cells and in the chemistry of the bulk solution, which together increase mineral supersaturation and promote carbonate precipitation (Schultze-Lam et al. 1996). A common indicator of this process is an increase in pH, often resulting from the production of CO_3^{2-} or HCO_3^- via bacterial ammonification (Stocks-Fischer et al. 1999) or from sulfate reduction under anoxic conditions (Van Lith et al. 2003). In addition, alkalization may also arise from photosynthetic activity, in which bacteria consume HCO_3^- and release OH^-, further promoting carbonate precipitation (Ferris et al. 1997). In contrast, active nucleation occurs when the negatively charged functional groups on bacterial cell walls or within extracellular polymeric substances (EPS) directly bind calcium ions, providing nucleation sites for $CaCO_3$

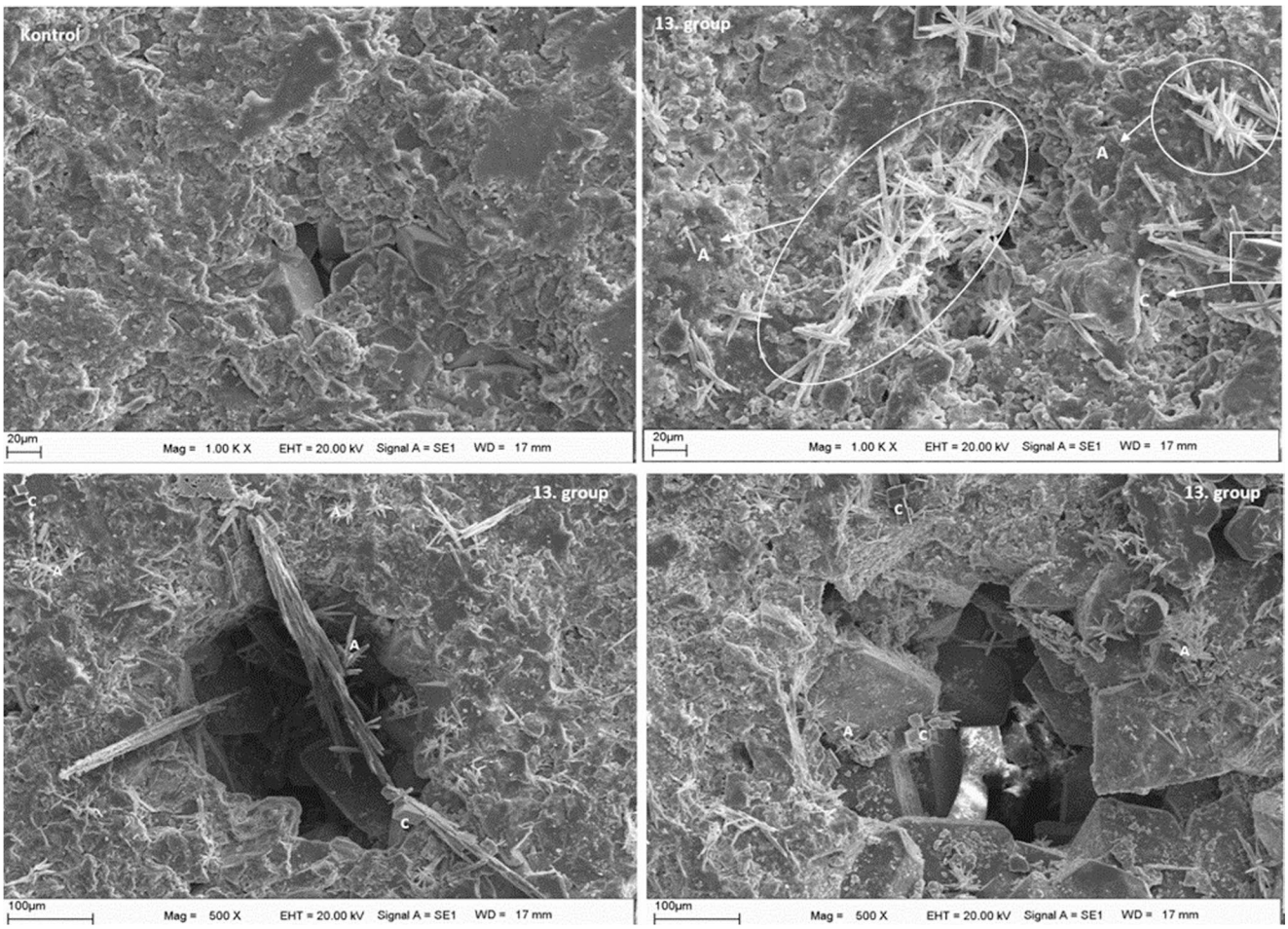

Fig. 12 SEM images of marble surfaces from the CO_2-untreated control group and $CaCO_3$ crystals formed on CO_2-untreated marble surfaces treated with dead bacteria and incubated in $CaCl_2$+U medium (group 13). C, calcite; A, aragonite

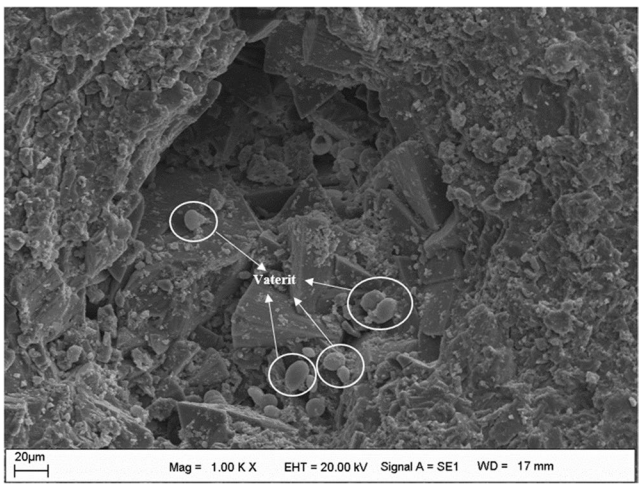

Fig. 13 SEM image of CO_2-untreated marble surfaces treated with dead bacteria in CaAcetate-GYE+U medium (group 12)

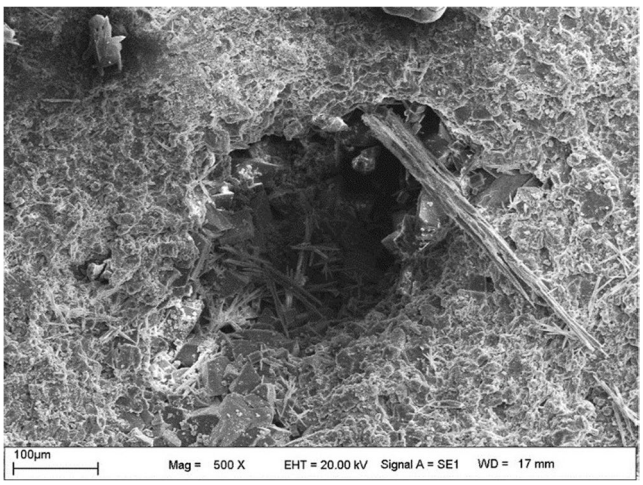

Fig. 14 SEM image of CO_2-untreated, bacteria-free marble surfaces incubated in $CaCl_2$+U medium (group 9)

crystal growth (Schultze-Lam and Beveridge 1994; Warren et al. 2001; Hoffmann et al. 2021). This mechanism reflects the direct involvement of microbial cell surfaces in mineral precipitation and complements the indirect biochemical changes associated with passive nucleation. In the present study, SEM-EDX and microscopic observations indicate

Table 2 Summary of crystal size, polymorph type, and biohealed area characteristics observed on marble surfaces under different bacterial, calcium source, and CO_2 pre-treatment conditions

CO_2 Application	Calcium Source	Bacterial Form	Crystal Size (μm)	Crystal Type	Biohealed Area Size
Present	$CaCl_2$+U	Live	20–100	Calcite, Aragonite	0.214 mm (diameter); 0.059 mm (diameter); 0.033 × 0.062 mm²; 0.031 × 0.066 mm²; macropores ~ 3 × 5 mm
Present	$CaCl_2$+U	Dead	10–20	Calcite, Aragonite	0.036 mm (diameter)
Present	CaAcetateGYE	Live	1–10	Vaterite	—
Present	CaAcetateGYE	Dead	1–10	Vaterite	—
Absent	$CaCl_2$+U	Live	10–20	Aragonite	—
Absent	$CaCl_2$+U	Dead	10–20	Calcite, Aragonite	—
Absent	CaAcetateGYE	Live	—	—	—
Absent	CaAcetateGYE	Dead	1–10	Vaterite	—

"—" indicates that no measurable biohealed area was detected under the corresponding experimental conditions. Biohealed area size refers to the dimensions of $CaCO_3$-filled regions determined from stereomicroscopic and SEM observations.

Table 3 XRD peak positions, d-spacings, relative intensities, and crystallographic plane assignments for calcite identified in the diffractogram shown in Fig. 15

Peak	2θ (°)	d (Å)	Relative intensity	Phase	(hkl)
1	23.1	3.85	20–25	Calcite	(012)
2	29.4	3.04	100	Calcite	(104)
3	31.4	2.85	15–20	Calcite	(006)
4	36.0	2.49	20–25	Calcite	(110)
5	39.4	2.28	35–45	Calcite	(113)
6	43.1	2.10	20–30	Calcite	(202)
7	47.5	1.91	15–25	Calcite	(018)
8	48.5	1.88	20–30	Calcite	(116)
9	57.5	1.60	15–20	Calcite	(122)
10	60.7	1.53	10–15	Calcite	(214)
11	61.0	1.52	8–12	Calcite	(300)
12	65.3	1.43	10–15	Calcite	(125)

surface-associated $CaCO_3$ formation, suggesting that such cell-mediated interactions may contribute to the observed mineralization alongside solution-driven processes.

According to EDX analysis, a higher carbon content was detected on the surface of marble samples from the CO_2-pre-treated control group. This observation suggests that pre-incubation of marble surfaces under CO_2 conditions increases surface-associated inorganic carbon, which may facilitate subsequent $CaCO_3$ nucleation. This interpretation is consistent with previous studies reporting that CO_2 exposure can modify surface chemistry and influence carbonate precipitation processes (Shirakawa et al. 2015). Similarly,

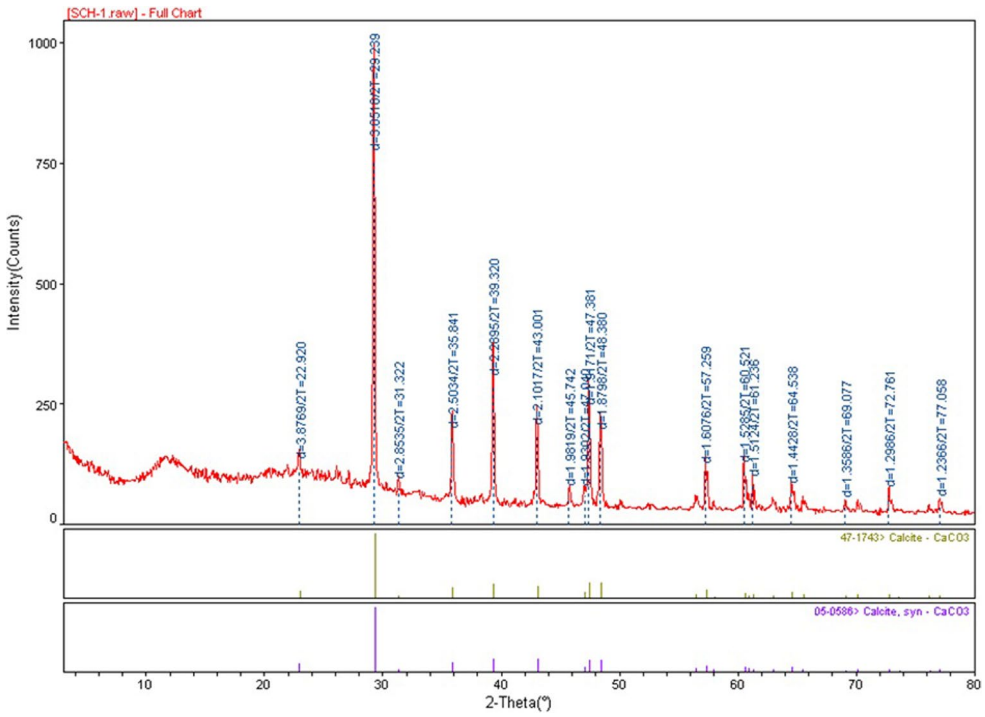

Fig. 15 X-ray diffraction (XRD) pattern of calcium carbonate crystals extracted from the macropores of CO_2-pre-treated marble surfaces incubated in $CaCl_2$+U medium (group 4)

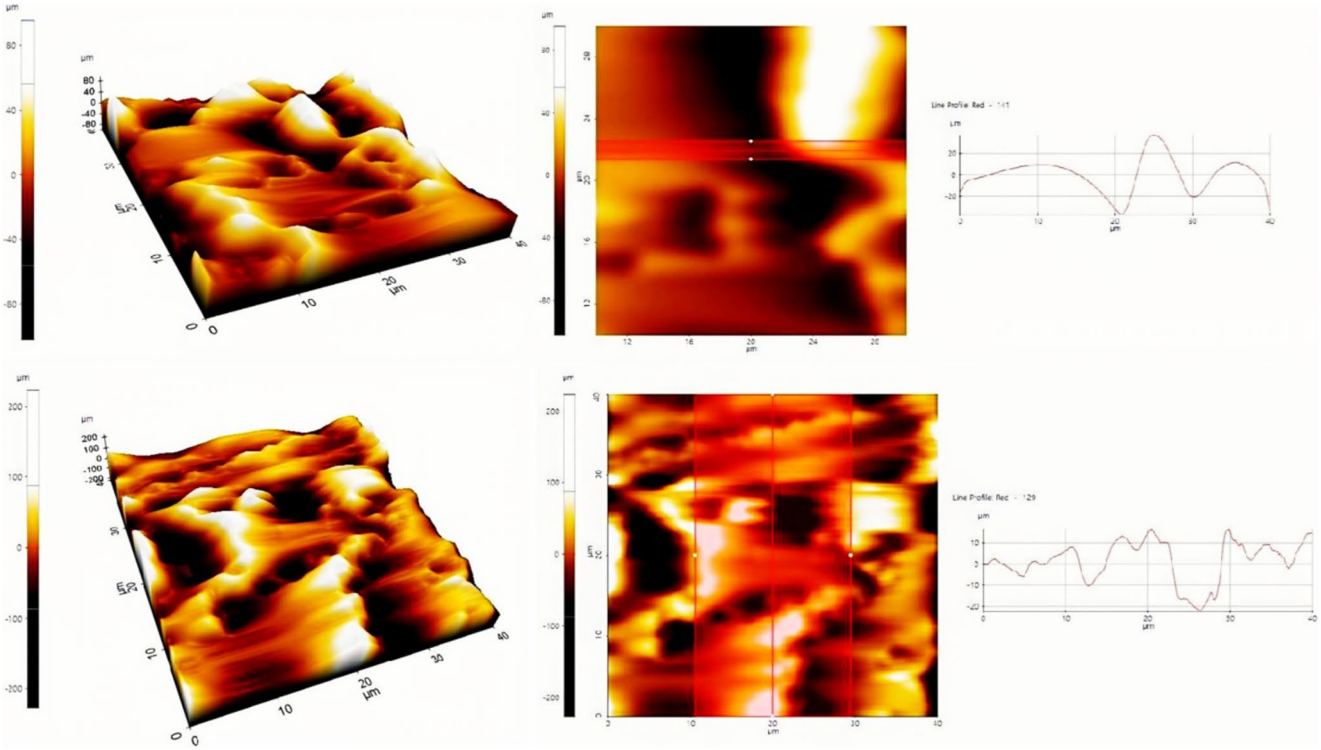

Fig. 16 AFM images of CO_2-pre-treated marble surfaces from the control group (group 7, top) and marble surfaces treated with live bacteria (group 4, bottom). Representative line profile analyses were used to determine the maximum pore/crack depth, defined as the vertical height difference between the bottom of surface pores or cracks and the adjacent intact marble surface

Isar (2020) reported that biocalcite formation is associated with the presence of Ca, O, C, and N in the surrounding environment, while Polat (2019) identified $CaCO_3$ formation based on elemental compositions including C, O, Na, Al, Si, K, Ca, and Ti.

Crystallization observed on surfaces associated with dead bacterial cells can be attributed to surface-mediated active nucleation mechanisms. The electronegative charges present on bacterial cell surfaces act as effective substrates for nucleation (Warren et al. 2001), although the underlying process differs from $CaCO_3$ precipitation driven by HCO_3^- production in metabolically active cells. In this context, chemically heterogeneous macromolecules on bacterial surfaces generate net negative charges that adsorb Ca^{2+} ions and subsequently attract CO_3^{2-} or HCO_3^- ions, thereby initiating $CaCO_3$ nucleation (Stocks-Fischer et al. 1999; Warren et al. 2001; Hoffmann et al. 2021). This surface-associated pathway is widely recognized as active nucleation (Van Lith et al. 2003). Furthermore, carboxyl groups present on the surfaces of both Gram-positive and Gram-negative bacteria exhibit spatial configurations homologous to those of calcite lattice planes and carbonate ions, facilitating active calcite formation (Braissant et al. 2003). Recent nanoscale studies have further demonstrated that substrate mineralogy, biofilms, and extracellular polymeric substances (EPS) strongly influence bacterially induced carbonate mineralization, highlighting EPS as an additional nucleation matrix beyond cell wall functional groups (Dubey et al. 2025). In contrast, crystallization observed on surfaces completely devoid of bacterial cells is more appropriately explained by abiogenic calcification or by organic matrix-mediated nucleation processes rather than cell-driven active nucleation.

These findings suggest that CO_2 pre-treatment functions as an effective surface-conditioning step by increasing inorganic carbon availability at the marble interface, which may promote local Ca^{2+}–CO_3^{2-} supersaturation and facilitate stable $CaCO_3$ nucleation during microbial activity. This interpretation is consistent with previous studies demonstrating that shifts in carbonate equilibria strongly influence $CaCO_3$ polymorphism and phase stability. Moreover, the distinct $CaCO_3$ polymorphs observed in samples treated with live and dead bacterial cells can be attributed to differences in local supersaturation conditions and nucleation pathways, as variations in surface chemistry are known to govern the preferential formation of calcite, aragonite, or vaterite (Liendo et al. 2022).

Overall, the findings of this study indicate that microbially induced carbonate precipitation mediated by *B. subtilis* ATCC 6633 represents a promising approach for marble biohealing. By modulating bacterial viability, calcium

source, and CO_2 pre-treatment conditions, $CaCO_3$ polymorphism and pore-filling behavior can be influenced, providing valuable insights for future applications in material conservation and durability enhancement; however, further studies are required to assess the long-term durability of the biocalcified layers under outdoor environmental conditions.

Conclusion

This study demonstrates that *B. subtilis* is capable of inducing effective biocalcification on marble surfaces, resulting in partial filling of both micro- (0.02–0.03 mm) and macro-pores (3–5 mm). The combination of live bacterial cells with CO_2 pre-treatment yielded the most extensive and stable $CaCO_3$ deposition, predominantly in the form of calcite and aragonite, whereas dead bacterial cells and calcium acetate favored the formation of less stable vaterite. These findings underscore the critical roles of bacterial viability and calcium source in governing $CaCO_3$ polymorphism and overall biohealing efficiency.

Beyond its mechanistic insights, this eco-friendly and sustainable approach offers a promising alternative for marble conservation and related biomineralization-based applications. By enabling the filling of natural pores and cracks, including regions that are difficult to access using conventional restoration techniques, microbially induced carbonate precipitation (MICP) represents a viable strategy for enhancing the durability of marble surfaces. Moreover, this work contributes to a broader understanding of microbial roles in carbonate mineralization and supports the development of low-impact conservation technologies aligned with contemporary sustainability and reduced carbon-emission goals.

Acknowledgements For the essential research facilities, we thank Inonu University Scientific Research Projects Management Unit (ISPMU).

Author contributions Conceptualization and design: SCY, AG, FNK-Methodology: SCY, TB, AGAnalysis and data interpretation: TB, FNK, SCYWriting original draft: SCYWriting original manuscript: SCY, AGAll authors read and approved the final manuscript.

Funding Open access funding provided by the Scientific and Technological Research Council of Türkiye (TÜBİTAK). This study is a part of a project (Project no: FYL-2021-2388) and supported by Inonu University Scientific Research Projects Management (BAP) Unit.

Data availability No datasets were generated or analysed during the current study.

Declarations

Ethical approval There are no studies by any of the writers in this article that used humans or animals as subjects.

Competing interests The authors declare no competing interests.

Open Access This article is licensed under a Creative Commons Attribution 4.0 International License, which permits use, sharing, adaptation, distribution and reproduction in any medium or format, as long as you give appropriate credit to the original author(s) and the source, provide a link to the Creative Commons licence, and indicate if changes were made. The images or other third party material in this article are included in the article's Creative Commons licence, unless indicated otherwise in a credit line to the material. If material is not included in the article's Creative Commons licence and your intended use is not permitted by statutory regulation or exceeds the permitted use, you will need to obtain permission directly from the copyright holder. To view a copy of this licence, visit http://creativecommons.org/licenses/by/4.0/.

References

Achal V, Pan X (2014) Influence of calcium sources on microbially induced calcium carbonate precipitation by *Bacillus* sp. CR2. Appl Biochem Biotechnol 173(1):307–317

Ahmad MA, Zhang J, Bing L, Tan P, Deng X (2024) Unlocking the efficacy of cement-shell encapsulation for microbial self-healing process of concrete cracks. J Mater Res Technol 32:2733–2742

Alvarado-Mata LY, Sánchez-Lozano JM, de la Cervantes- Torre JI, Álvarez-Valdez AR, Salinas-Mireles JP, Chávez Hita-Wong AY, Castro-Alonso María José, Luévanos-Escareño Miriam Paulina, Narayanasamy Rajeswari, Balagurusamy N (2025) Advances in microbially induced carbonate precipitation metabolic pathways and regulatory mechanisms for bioconcrete development. J Sustain Cement-Based Mater. https://doi.org/10.1080/21650373.2025.2525559

Anbu P, Kang C-H, Shin Y-J, So J-S (2016) Formations of calcium carbonate minerals by bacteria and its multiple applications. Springerplus 5(1):1–26

Bozbeyoğlu NN, Sensoy Candogan T, Arslan Ş, Kabalay B, Bozkaya Ö, Akyol E, Mercan Doğan N (2020) Calcium carbonate precipitation by urease and carbonic anhydrase. Pamukkale Univ J Eng Sci 26(3):513–518

Braissant O, Cailleau G, Dupraz C, Verrecchia EP (2003) Bacterially induced mineralization of calcium carbonate in terrestrial environments: the role of exopolysaccharides and amino acids. J Sediment Res 73:485–490

Colao F, Fantoni R, Lazic V, Morone A, Santagata A, Giardini A (2004) Libs used as a diagnostic tool during the laser cleaning of ancient marble from mediterranean areas. Appl Phys A 79(2):213–219

De Muynck W, De Belie N, Verstraete W (2010) Microbial carbonate precipitation in construction materials: a review. Ecol Eng 36(2):118–136

Down JL, MacDonald MA, Tétreault J, Williams RS (1996) Adhesive testing at the Canadian conservation institute: an evaluation of selected poly(vinyl acetate) and acrylic adhesives. Stud Conserv 41(1):19–44

Dubey AA, Toprak P, Pring A et al. (2025) Effect of substrate mineralogy, biofilm and extracellular polymeric substances on bacterially induced carbonate mineralisation investigated with in situ nanoscale ToF-SIMS. Sci Rep 15:29368. https://doi.org/10.1038/s41598-025-14083

Feng B, Yong AK, An H (2007) Effect of various factors on the particle size of calcium carbonate formed in a precipitation process. Mater Sci Eng A 445–446:170–179. https://doi.org/10.1016/j.msea.2006.09.010

Ferris FG, Thompson JB, Beveridge TJ (1997) Modern freshwater microbialites from Kelly Lake, British Columbia, Canada. Palaios. https://doi.org/10.2307/3515423

Gorospe CM, Han SH, Kim SG, Park JY, Kang CH, Jeong JH, So JS (2013) Effects of different calcium salts on calcium carbonate

crystal formation by *Sporosarcina pasteurii* KCTC 3558. Biotechnol Bioprocess Eng 18(5):903–908
Hammes F, Boon N, de Villiers J, Verstraete W, Siciliano SD (2003) Strain-specific ureolytic microbial calcium carbonate precipitation. Appl Environ Microbiol 69(8):4901–4909
Hargis CW, Telesca A, Monteiro PJM (2014) Calcium sulfoaluminate (Ye'elimite) hydration in the presence of gypsum, calcite, and vaterite. Cem Concr Res 65:15–20. https://doi.org/10.1016/j.cemconres.2014.07.004
Hoffmann TD, Reeksting BJ, Gebhard S (2021) Bacteria-induced mineral precipitation: a mechanistic review. Microbiology (Reading, Engl.) 167(4):001049
Isar A (2020) Design of cementitious composites with improved microstructural properties through bacterial biomineralization (Master's thesis). Ege University, Institute of Science, Izmir
Kart NNB (2021) Interaction of ureolytic bacteria and clay in bacterial calcium carbonate mineralization: *Paenibacillus favisporus* U3 (Doctoral dissertation). Pamukkale University, Institute of Science, Denizli
Keren-Paz A, Maan H, Karunker I, Olender T, Kapishnikov S, Dersch S, Kartvelishvily E, Wolf SG, Gal A, Graumann PL, Kolodkin-Gal I (2022) The roles of intracellular and extracellular calcium in *Bacillus* subtilis biofilms. iScience 25(6):104308. https://doi.org/10.1016/j.isci.2022.104308
Li Y, Li Y, Ma H, Li J (2024) The hydration, microstructure, and mechanical properties of vaterite calcined clay cement (VC3). Cem Concr Res 175:107374. https://doi.org/10.1016/j.cemconres.2023.107374
Liendo F, Arduino M, Deorsola FA, Bensaid S (2022) Factors controlling and influencing polymorphism, morphology and size of calcium carbonate synthesized through the carbonation route: a review. Powder Technol 398:117050. https://doi.org/10.1016/j.powtec.2021.117050
Liu Q, Liu Y, Zeng K, Yang F, Zhu H, Liu Q (2011) Advanced design of Chinese traditional materials for the conservation of historic stone buildings. J Archaeol Sci 38:1896–1900
Luhar S, Luhar I, Shaikh FUA (2022) A review on the performance evaluation of autonomous self-healing bacterial concrete: mechanisms, strength, durability, and microstructural properties. J Compos Sci 6(1):23
Mann S (2001) Biomineralization: Principles and Concepts in Bioinorganic Materials Chemistry. Oxford, New York
Moropoulou A, Zendri E, Ortiz P, Delegou ET, Ntoutsi I, Balliana E, Becerra J, Ortiz R (2019) Scanning microscopy techniques as an assessment tool of materials and interventions for the protection of built cultural heritage. Scanning 2019:5376214. https://doi.org/10.1155/2019/5376214
Naidu S, Blair J, Scherer GW (2016) Acid-resistant coatings on marble. J Am Ceram Soc 99(10):3421–3428
Polat B (2019) Investigation of self-healing of geopolymer mortar using microorganisms (Doctoral dissertation). Istanbul University-Cerrahpaşa, Department of Civil Engineering, Istanbul
Qafoku NP, Lawter AR, Gillispie EC, McElroy E, Smith FN, Sahajpal R, Cantrell K, Freedman V (2022) Calcium carbonate minerals as scavengers of metals and radionuclides: Their role in natural attenuation and remediation. In: Sparks DL (ed) Advances in Agronomy, vol 176, pp 115–147
Rajasekar A, Zhao C, Wu S, Murava RT, Wilkinson S (2024) Synergistic biocementation: harnessing *Comamonas* and *Bacillus* ureolytic bacteria for enhanced sand stabilization. World J Microbiol Biotechnol 40(7):229. https://doi.org/10.1007/s11274-024-04038-3
Ramakrishna C, Thenepalli T, Huh JH, Ahn JW (2016) Preparation of needle like aragonite precipitated calcium carbonate (PCC) from dolomite by carbonation method. J Korean Ceram Soc 53(1):7–12
Raza A, Khushnood RA (2022) Bacterial carbonate precipitation using active metabolic pathway to repair mortar cracks. Mater Basel 15(19):6616
Robles-Fernández A, Areias C, Daffonchio D, Vahrenkamp VC, Sánchez-Román M (2022) The role of microorganisms in the nucleation of carbonates, environmental implications and applications. Minerals 12(12):1562
Schultze-Lam S, Beveridge TJ (1994) Physicochemical characteristics of the mineral-forming S-layer from the Cyanobacterium *Synechococcus* strain GL24. Can J Microbiol 40(3):216–223
Schultze-Lam S, Fortin D, Davis BS, Beveridge TJ (1996) Mineralization of bacterial surfaces. Chem Geol 132(1–4):171–181
Seifan M, Samani A, Berenjian A (2016) Induced calcium carbonate precipitation using Bacillus species. Appl Microbiol Biotechnol 100:9895–9906. https://doi.org/10.1007/s00253-016-7701-7
Shirakawa MA, John VM, De Belie N, Alves JV, Pinto JB, Gaylarde CC (2015) Susceptibility of biocalcite-modified fiber cement to biodeterioration. Int Biodeterior Biodegrad 103:215–220
Siddique R, Chahal NK (2011) Effect of ureolytic bacteria on concrete properties. Constr Build Mater 25(10):3791–3801
Sreekala AGV, Nair S, Nathan VK (2024) Microbially induced calcium carbonate precipitation using *Lysinibacillus* sp.: a ureolytic bacterium from Uttarakhand for soil stabilization. Curr Microbiol 81(11):387. https://doi.org/10.1007/s00284-024-03899-z
Stocks-Fischer S, Galinat JK, Bang SS (1999) Microbiological precipitation of CaCO3. Soil Biol Biochem 31(11):1563–1571. https://doi.org/10.1016/S0038-0717(99)00082-6
Su Y, Liu C, Fang H, Zhang D (2020) *Bacillus subtilis*: a universal cell factory for industry, agriculture, biomaterials and medicine. Microb Cell Fab 19:173
Sumathi A, Murali G, Gowdhaman D, Amran M, Fediuk R, Vatin NI, Deeba Laxme R, Gowsika TS (2020) Development of bacterium for crack healing and improving properties of concrete under wet–dry and full-wet curing. Sustainability 12(24):10346
Tai CY, Chen FB (1998) Polymorphism of CaCO<Subscript>3</Subscript>, precipitated in a constant-composition environment. AIChE J 44(8):1790–1798
Tourney J, Ngwenya BT (2009) Bacterial extracellular polymeric substances (EPS) mediate CaCO3 morphology and polymorphism. Chem Geol 262(3–4):138–146
Van Lith Y, Warthmann R, Vasconcelos C, McKenzie JA (2003) Microbial fossilization in carbonate sediments: a result of the bacterial surface involvement in dolomite precipitation. Sedimentology 50(2):237–245
Wang J, Becker U (2009) Structure and carbonate orientation of vaterite (CaCO<Subscript>3</Subscript>). Am Mineral 94(2–3):380–386
Warren LA, Maurice PA, Parmar N, Ferris FG (2001) Microbially mediated calcium carbonate precipitation: implications for interpreting calcite precipitation and for solid-phase capture of inorganic contaminants. Geomicrobiol J 18(1):93–115
Wiktor V, Jonkers HM (2011) Quantification of crack-healing in novel bacteria-based self-healing concrete. Cem Concr Compos 33(7):763–770. https://doi.org/10.1016/j.cemconcomp.2011.03.012
Zhang Y, Guo HX, Cheng XH (2014) Influences of calcium sources on microbially induced carbonate precipitation in porous media. Mater Res Innov 18(2):2–79
Zhong M, Liu B, Zhang L, Wang J, Chen J, Li J, Liu Y, Ming L (2022) Experimental study on microbial induced calcium carbonate precipitation to enhance reservoir recovery. Iran J Biotechnol 20(1):46–55
Zhu T, Dittrich M (2016) Carbonate precipitation through microbial activities in natural environment, and their potential in biotechnology: a review. Front Bioeng Biotechnol 4:4. https://doi.org/10.3389/fbioe.2016.00004
Luo M, Ji A, Li X, Yang D (2024) Performance evaluation of self-healing recycled concrete using biomineralization modified recycled aggregate as bacterial carrier. Journal of Building Engineering 86:109000. https://doi.org/10.1016/j.jobe.2024.109000

Publisher's Note Springer Nature remains neutral with regard to jurisdictional claims in published maps and institutional affiliations.